Feasibility Study of Wearable Sweat Sodium Sensor

By

Tianchi Zhang, Master of Engineering(Biomedical)

Supervisor: Youhong Tang

Date of Submission:

29th May 2020

Submitted to the College of Science and Engineering in partial fulfilment of the requirements
for the degree of Master of Engineering (Biomedical) at Flinders University, Adelaide,
Australia

Acknowledgement

First of all, I would like to thank my supervisor Professor Youhong Tang, who used his professional and rigorous academic style to help me complete this thesis. He gave many effective suggestions and improvements, which made my work completed quickly and efficiently.

Secondly, I would like to thank the engineers in the JRC (Joint Research Centre for Personal Health Technologies) Flinders Group for their help. Dr. Angus Wallace, Ms. Xinyi Zhang helped me on the arrangement and management of research. Mr. Hao Fu and Mr. Anh Anderson Pham helped me in the fields of electronic engineering and single chip microcomputer. Thanks also to the Flinders University Engineering Services staff and Flinders Analytical staff for their help.

Finally, I want to thank my parents and partners for their encouragement and support in the process of completing the master thesis.

Declaration

I certify that this work does not contain any materials previously submitted for applying for degrees or diplomas at any university; to the best of my knowledge and belief, it does not contain any materials previously published or written by others unless there is an appropriate reference in the text.

Tianchi Zhang

April 2020

Abstract

In this study, a new wearable sweat sensor has been introduced. Unlike traditional medical wearable devices, which detect physical information such as pulse or heart rate by physical or mechanical, this new type of wearable device is a real-time biochemical information collection device that can quantitate the concentration of sodium ions from human sweat. Through quantitative analysis of the content of sodium ions in sweat, to infer the health status of the human body.

In this project, the properties of three different types of electrodes were tested. These three kinds of electrodes are saturated calomel electrode, screen-printed electrode and modified electrode. They can all react with the free ions in the solution and detect the potential released when the ions undergo a redox reaction. But they all have their own characteristics and properties. These three electrodes have been analysed and selected modified electrodes have been selected as the most suitable electrode to use on this new type of wearable device.

Firstly, the three electrodes were subjected to an electrochemical reaction under the same conditions. The electrodes were connected to an AUTOLAB electrochemical workstation. Observing the results of the open circuit potential (OCP), it was found that the modified electrode can specifically react with sodium ions in sodium chloride solution, and only the potential of the sodium ion reduction reaction is detected on the working electrode. And its small size makes it suitable as part of wearable devices.

Secondly, using the relevant knowledge of signal processing, a functional circuit is designed to collect and process the signals received by the electrodes. This circuit contains a voltage buffer circuit, a subtractor differential amplifier circuit and a 4th order low-pass Butterworth filter circuit. After simulating the designed circuits, Altium Designer is used to make a printed circuit board (PCB), and then the components of the circuit board are soldered. After the soldering is completed, it is connected to the electrode for testing.

An assembled device connected by functional circuits, electrodes and LED modules driven by Arduino can form a complete system. It can be used to detect, process and display microampere-level electrochemical signals. This provides feasibility for the detection of the electrochemical properties of substances in human body fluids.

CONTENT

Contents of Figure

Contents of Table

Chapter 1 Introduction

This chapter gives the motivation of the master's thesis topic, and then introduces the research background and related theory of the project. Finally, it demonstrates the research methodology and the outline of the thesis.

1.1 Motivation of the Master Thesis

In today's society, with the continuous improvement of the medical level of science and technology, and the growing demand for understanding and attention to their own health. In the fast-paced life, the use of daily scattered time and simple and convenient methods and equipment to monitor physiological indicators is the current development direction of medical equipment.

The rise and development of many wearable devices nowadays also confirm this. And the phenomenon that can be seen is that more and more companies have begun to get involved in this convenient and fast wearable device, such as Apple Watch which can monitor heart rate in real time. They all have the common characteristics of small size, simple operation and quick response. Different from the traditional monitoring instruments or methods in hospitals, for this wearable or portable instrument, it is more in the scope of rapid test results and results are only a preliminary judgment or reference purpose. It is different from the precise diagnosis of hospital equipment.

Most of the existing portable or wearable devices on the market mostly detect the primary physiological response of heart rate based on the principles of physical vibration. And it involves the detection of body fluids, but the detection of blood glucose content is the most common. In order to detect biochemical information in blood, the device must be invasive to collect blood samples. As an equally important body fluid, sweat is also rich in biological information, and the collection of sweat is more convenient than blood or other body fluids.

Cystic fibrosis, as a common genetic disease, is very important for its detection and monitoring. The content of sodium ions in body fluids is used as an indicator for the detection of cystic fibrosis. Quantitative analysis of sodium ions in body fluids has become a field of great medical significance and commercial prospect. Sweat, as an easily obtained body fluid, also contains a certain amount of sodium ions, and it has certain significance for the analysis of the content of sodium ions in sweat. This is also the purpose and motivation of my master thesis.

The project of my master thesis is dedicated to the development of a new type of wearable device, which is different from the existing wearable device that only analyses the physiological state of the human body based on physical reactions, but based on chemical analysis to carry out quantitative analysis of the substances in sweat and health monitor. But strictly speaking, my project is just a feasibility study, which integrates multiple knowledge points and integrates the characteristics and needs of each part according to needs to serve my project. To show that based on the theory of a wearable device, the knowledge I have learned can be integrated. The specific content and knowledge points involved will be elaborated in the next section.

1.2 Background and Basic Theories

1.2.1 Electrochemistry

This project is based on the theory of electrochemistry and image processing. Electrochemical theory is the first part of the project, collecting sodium ion chemical signals from human sweat (laboratory simulated sweat solution). The ion concentration in the solution can be converted into an open circuit voltage and collected and stored. In an ideal environment, this open circuit voltage has a relationship with the ion concentration in the solution. For the determination of the ion concentration in the solution, based on the knowledge of electrochemistry, there are already many equipment working in the laboratory environment that can measure the open circuit voltage of a certain ion of the solution. In this project of mine, I use the AUTOLAB electrochemical workstation of Metrohm Medical Equipment Company. The working principle and result collection of this workstation will be described in detail below.

1.2.2 Signal Processing

Another part of my project is to process the signals collected by the first part. And this part involves knowledge of electronics and circuits. Because the concentration of sodium ions in sweat is very low, the concentration of sodium ions in sweat is on the order of millimolar. Such a concentration causes its corresponding open circuit voltage to be in the order of millivolts. For such a tiny electrochemical signal, it needs to be amplified to a level that can be collected, however, during the amplification process, there will be distortion. Therefore, how to ensure that the original signal state is not lost or amplified or transposed into an electrical signal that can be processed is what I need to work. Filtering the noisy of original signal is also part of the project work. The design of the filter circuit is based on the characteristics and functions of the Butterworth filter. And this part will be based on software simulation and hardware production. For software simulation, the circuit needs to be designed and manufactured on NI MultiSIM 14, and the software also has the function of simulation. It is necessary to emulate the software before making the hardware to determine its functionality and then make the hardware. For hardware production, it is necessary to draw a schematic diagram on Altium Designer 19 and convert it into a PCB package diagram, and then print the PCB package diagram into a PCB board. After the production of the PCB board is completed, the electronic components on the board need to be soldered. For this part, it is a key point of my project, spending a lot of time on both software and hardware.

1.2.3 Display and Package

The display part involves programming and microcontroller basics because I used a microcontroller to drive an LED display module to display the final output. I use Arduino Neo for single chip microcomputer, which is used for digital to analog converter. The microcontroller and LED display program will also be introduced in the following chapters.

After completing a series of tasks, I used 3d printing technology to print a shell for all parts. The top of the shell has a part for the LED module to display, and the bottom is a part that contacts the human skin. After completion, assemble it up. The 3D printing is based on the prototype produced by Spaceclaim software.

1.3 Methodology and Outline of my Research

My research is divided into six parts.

The first part is a literature review, through a large number of documents to understand the basics of wearable devices and electrochemistry. Because I did not learn the knowledge of electrochemistry during my undergraduate course, including my master's degree. So, I must master some basic electrochemical knowledge before starting my research. Including the generation of open circuit voltages on the electrodes, these are shown in the basic electrochemical section in Chapter 2.

The second part is to select suitable electrodes for my research project based on the basis of electrochemistry. The electrode is used as a tool to convert chemical signals stored in ions in sweat into electrical signals. The selection of electrodes is a very important role. There are many types of commercial electrodes on the market, with different types modifications. Choosing an electrode that can detect the content of sodium ions in sweat from these electrodes is the beginning of my research project. The electrode has not been selected properly, and the next project will not be able to proceed. For different electrodes, I have conducted horizontal evaluations, that is, performing chemical experiments on different types of electrodes under exactly the same conditions to find out their respective advantages and disadvantages.

The third part is to process the electrical signal collected by the electrode after selecting the electrode. I used the method of software simulation first, and then hardware development. First use the software on the computer for modelling, introduce analog signals, and observe the output signals. The hardware development is based on the most common printed circuit board (PCB) production, using Altium Designer to design and develop the circuit. The soldering of the circuit board is done in the laboratory with a solder gun.

The fourth part is the design of the result part. Because the sodium ion concentration in sweat is low, the electrochemical signal is weak, and the LED element cannot be directly used to display the final digital result of the open circuit voltage. In this case, an external MCU is needed to drive an Arduino professional 4-digit 7 segments LED display module. The editing of related programs will also be introduced in a dedicated chapter 7.

The fifth part is the analysis and discussion of the results. Because the content of sodium ions in sweat is very small, the error when conducting experiments sometimes exceeds the difference caused by its own concentration difference. My research topic is the feasibility analysis of the sodium ion sensor in sweat, which proves that under the premise of various theoretical supports, the method of electrochemical ion detection can be used to quantitatively analyse the content of a specific substance in an unknown concentration solution. It also shows that my research project has very broad prospects.

The six part is future work that is expected to place all the components in a special box. As for the production of the box, 3D printing technology will be used to print a shell that perfectly fits all parts. And this part is also a big challenge for me who has never been exposed to 3D printing technology. Furthermore, the soft, flexible substance of thermoplastic polyurethane (TPU) and nano-silver ink through the Diamitx Material Printer. These works should have been completed within the study period, but due to time limitation and the impact of the current situation. These tasks will be completed in the future.

Table 1 Components of whole research

Components	Quantities	Comments
Saturated Calomel Electrode	2	It is made of ceramics and has been damaged, but its value is not high.
Platinum mesh electrode	1	The chemical properties are lively and expensive.
Carbon rod	1	As courter electrode, stable and has no influence to results.
Screen-printed electrode	50	The cost is not high and the plasticity is strong. You can use it as a substrate to make my own modified electrode.
Modified SPE	1	Expensive(160 AU dollars), binds specifically to sodium ions in solution and produces the expected result

Printed Circuit Board	6	Produced by Flinders University Engineering Services.
Chip capacitors and chip resistors	30	Small size and cheap price (purchased from China)
OP AMP LT1462	12	25 AU Dollars each. Perfect for my research project (Detailed introduction in special chapters)
Arduino Power Supply Module	1	Boost 9V battery to 10V (LT1462 working voltage) and keep it unchanged
Arduino Uno Microcomputer	1	See chapter 7 for details
4 bits 7 Segment LED display module	1	See chapter 7 for details

Chapter 2 Literature Review

This chapter will state a general summary of all the literature about the wearable sensor and its theory and experiment. I will initiate it with detection of ingredients in sweat based on the wearable technologies; then expansion in the field of electrochemistry through comparing several types of different electrode patch or array which can recognize and quantitate the ions in perspiration. Finally, it will enumerate several methods of output of bio-signal while what I used is voltage signal.

2.1 Ingredients Testing of Human Sweat

2.1.1 Various Ingredients in Human Sweat

Sweat is a common and easily accessible body fluid. Currently, sweat comprises various biomarkers of different diseases including cystic fibrosis and diabetes.[1] As the cystic fibrosis is examined by the content of sodium ion in sweat and diabetes relatives with the glucose which is existing diffusely in sweat and the testing technologies are highly developed. Furthermore, sweat also contains potassium ions, lactate. Potassium ion and sodium ion have same properties that both of them relates to the hemopathy and muscle spasm. Lactate can be an indicator of asthma and myasthenia. Glucose is broken down and oxidized to pyruvate, from which lactate is produced. Metabolic intermediates like these can be used as indicators of the environmental balance in the human body.[2]

Table 2 Ingredients in sweat

Composition	Description	Relative disease	Detective method
Na^+, K^+	Ions which are distributed in sweat widely.	Hyponatremia, hypokalemia and muscle cramps, etc.	ISEs (Ions Selective Electrode), PVB coated reference electrode.
Glucose	Metabolic intermediate, an indicator of a person's metabolic balance.	Diabetes.	GO_x (Glucose oxidase electrode) $Glucose + GO_x \Rightarrow Glucoxic\ acid$
Lactate	Glucose is broken down and oxidized to pyruvate, from	Muscle weakness and asthma.	LO_x (Lactate oxidase electrode)

	which lactic acid is produced.		$Lactate + LO_x \Rightarrow Pyruvate$
Temperature	Temperature of upper skin.	Skin injury such as ulcers.	Temperature electrode.

For my research, I chose sodium ion as the target ion. This is because sodium ions are ubiquitous ions in the laboratory and are relatively easy to prepare compared to other substances. And the sodium ion detection can directly use the corresponding sodium ion selective electrode, the detection conditions are simple.

2.1.2 Conventional Sweat Testing Methods

Different with conventional blood and urine testing, detection of anthropic perspiration is non-invasive and real-time continually controlling. The traditional sweat testing method is collecting sweat into a reagent bag, and using antigen-antibody, ion selective electrode or conductivity measurement to determine the organic metabolite and concentration of the ions. Nevertheless, these technologies are stuck in the laboratory environment rather than extending to the public. Various limitations of sweat as a clinical sample include: difficulty in producing sufficient sweat samples, evaporation of samples, lack of appropriate sampling devices, and lack of trained staff.[3]

2.1.3 Microfluidic Model

Around 2015, propose and establish of the bio-microfluidic model provides a fire-new feasibility for development of sweat testing.

The human eccrine sweat gland comprises several geometrically distinct portions, the secretory coil (diameter 5-40 μm), the dermal duct (diameter 10-20 μm), and the upper coiled duct (cuticula), as shown in Figure 2(a). The upper coiled duct is also often referred to as the acrosyringium. In this region, the sweat duct expands in diameter slightly, until it emerges at the surface of the skin.[4-5]

Based on the Poiseuille fluid theory:

$$R = \frac{128\mu L}{\pi d^4}$$

$$P = R * Q$$

$$Press = Flow\ Resistance * Volume\ Rate\ of\ Flow$$

Modelling:

The secretory coil can be regarded as a pressure source plus a flow resistance; the dermal duct and part of the upper coiled duct can be regarded as a flow resistance respectively; due to the surface tension and the convex curvature of the meniscus sweat, the skin outside can be regarded as a pressure source.

It provides a completed procedure of the detected signal and its bio-microfluidic model from blood to sweat and be collected by bio-sensor. It proves that the feasibility of connection between electrolyte, metabolite and concentration of corresponding substance in blood. It proves the possibility of efficient real-time biological sensing. Based on this theory, a large number of wearable devices and electrode arrays have been designed and researched, and they are expected to be applied to the human body.

2.1.4 Low-cost Wearable Devices

Wearable medical devices can collect human physiological data (such as blood glucose, blood pressure, heart rate, blood oxygen content, body temperature, breathing rate, etc.) through sensors, and wirelessly transmit the data to a central processing unit (such as a small handheld wireless device, etc.[6] A warning signal is issued when an abnormality occurs, and the central processor sends the data to the medical centre, so that the doctor can perform comprehensive, professional, and timely analysis and treatment. For example, non-invasive continuous monitoring of blood glucose, non-invasive continuous monitoring of blood pressure, and non-invasive continuous monitoring of blood oxygen. Wearable medical devices can monitor blood glucose, blood pressure, blood oxygen and other data not only with smartphones, but also use cloud storage technology to store and analyse monitoring data through the cloud, and connect with the hospital's medical record system and monitoring centre provide early warning and corresponding diagnosis and treatment advice in case of abnormality.[7] Wearable medical devices can be used not only for vital signs, but also for disease treatment. For example, non-invasive treatment technologies, including electrotherapy, magnetic therapy, ultrasound therapy, and transdermal drug delivery, have been research hotspots in recent years, and are also the key development directions of wearable therapy systems.

The global wearable medical devices market is expected to grow at a CAGR of 4.6% in the first half of the forecast period. In 2016, the wearable health & fitness devices submarket held 49% of the global wearable medical devices market. It is not difficult to see that wearable medical devices are gradually occupying market share, and low-cost wearable devices have become a trend of modern people's concern for health. And sweat detection equipment has become the focus of people's research due to its non-invasive and real-time characteristics.

Today's well-known wearable devices are based on ion-selective electrode theory or ion-selective membranes or ion-selective arrays which are developed and extended based on this theory. I will discuss the ion selective electrode in more detail later in the section on electrochemistry. This section will give a general current situation of wearable devices that is used to detect the bio-signal of human sweat.

2.2 Electrochemical Basics and Ion Selective Electrode

2.2.1 Electrochemistry and Nernst Equation

As expound previously, the most widespread technology of sweat testing is based on electrochemistry. Through an electrode, the biological signal which is hided in sweat is converted into a modifiable and unambiguous electrical signal. This entire process can occur because of the migration and change of location of various ions in the solution, and the migration of ions will drive the movement of electrons, which is the current. In addition, the movement of electrons causes a difference in potential at different locations, creating a voltage.8

To quantitate concentration of ions in solution, the open circuit potential is the most optimal indicator. Literally, it is seemed as the open circuit at the superhigh resistance where is not any current pass through the circuit. Actually, there are two currents with same magnitude and opposite direction. The positive current counteracts the negative current. In an ideal situation, a particular ion in a solution will generate a particular open circuit potential at equilibrium as known as standard electrode potential. In other words, each of these ions will generate a certain potential in the solution, and that potential will not change because of the state of the other ingredients in the solution, but because of the concentration of the ion itself. It can be expected that there is a linear relationship between ion concentration and open circuit potential:

$$E_{OCP} = \alpha + \beta \ln\left(C_{ions}\right)$$

The α and β are constants and the concentration of ion could be quantitated by measurable voltage signal. This equation can be seen as a form of Nernst Equation in solution.

Taking the detection of sodium ions in the solution as an example, there will be such a basic relationship in the solution:

$$Na^+ + e \rightarrow Na$$

And its Nernst Equation:

$$E_{Na^+} = E_0 + \frac{RT}{nF} \ln\left[Na^+\right]$$

However, even a pure sodium ion solution without other cation interference will inevitably have another reaction to affect the expected output.

$$H^+ + e \rightarrow H_2 \uparrow$$

It occurs extensively and can be detected by unmodified electrodes. It is the reason why the electrode used for ion detection needs modification. Not only that, the reduction of sodium ions to solid sodium will react with the water in the solution.

$$Na + H_2O \rightarrow Na^+ + H_2 \uparrow$$

Therefore, the electrode cannot be used directly, it should be modified to only react to specific ions. The voltage is the potential difference between two different electrodes. Therefore, the electrodes used for detection cannot exist alone because this is a closed cell system.[13] Most of the current studies are three-electrode systems, and two-electrode systems also exist.

To reduce the influence of the chloride, the support electrolyte is required. As the open circuit potential is small, the resistance of the solution relates with the concentration of ions. The support electrolyte is required to have high concentration and no interference ions. The detected solution is dissolved by sodium chloride, the calcium chloride could be support electrolyte. And the concentration of $CaCl$ should be at least 100 time as NaCl solution.

2.2.2 Three-Electrode System and Potential Relationship

The three-electrode system is composed of a working electrode, a reference electrode and a counter electrode. When the electrode is working, the potential of the working electrode will change as the ion concentration changes. Because the working electrode is a very active metal, the polarization reaction occurs to a high degree on the working electrode. The reference electrode generally uses Ag /AgCl, which can keep the potential stable, and it will be described in detail in the potential relationship later. The existence of the counter electrode is to measure the polarization current, and the open circuit voltage what concerned about does not help much, so many studies only use the working electrode / reference electrode two-electrode system. A general electrochemical device will have a fourth support electrode in addition to the above three electrodes. However, the support electrode cannot be used as a reference electrode because it can also undergo polarization reaction and cannot be used as a fixed reference. Generally, the supporting electrode is connected to the working electrode.[9]

In January 2016, a research team from California Institution of Technology reported a fully integrated flexible wearable sweat sensor FISA (Flexible Integrated Sensor Array) based on plastic materials and silicon integrated circuits. This array uses a three-electrode system.[10]

As stated earlier, in order for this electrode to specifically react to specific ions or metabolites, it must be modified on the surface of the working electrode. The details about modification will be described in the next section. The surface of the working electrode is mostly covered with a selectively permeable membrane. In this case, there will be a schematic like this:

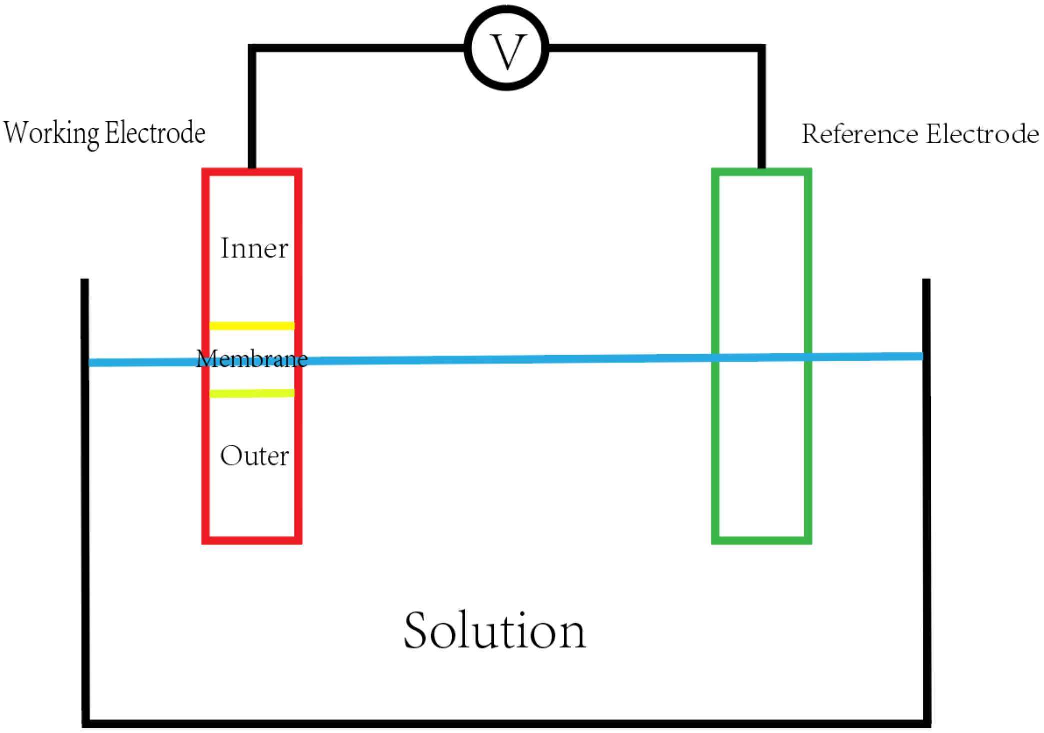

Figure 1 The Schematic of Two-Electrode System in Solution

As shown in the figure, there will be the following mathematical relationship:

$$E_{Reading} = E_{inner} - E_{reference} - E_{membrane} - E_{support\ Electrolyte}$$

$$E_{reference} = E^0_{Ag^+} + \frac{RT}{nF}\ln[Ag^+] = E^0_{Ag^+} + \frac{RT}{nF}\frac{\ln[Ag^+]\,[Cl^-]}{\ln\,[Cl^-]}$$

$$[Ag^+][Cl^-] = Ksp(AgCl)$$

Ksp is an abbreviation of solubility product constant.[11] Therefore, the $E_{reference}$ can be regarded as a constant. In the model of concentration change, the working electrode potential is also constantly changing, so $E_{reference}$ can be regarded as 0.

The presence of the supporting electrolyte is to eliminate the interference of the anions present in the solution with the potential results. Because the magnitude of the open circuit potential is very small, and the resistance of the solution is related to the concentration of ions in the solution, it is necessary to support the electrolyte with a high concentration and no other anion interference. For example, if the sodium ion solution is dissolved from sodium chloride crystals, then the same anionic potassium chloride solution is needed as the supporting electrolyte, and the concentration of the potassium chloride solution is at least 100 times that of the sodium chloride solution.

E_{inner} is a constant as well because its value is equal to the potential generated by the electron movement when the cation is reduced after passing through the selective membrane. This value is constant in a fixed concentration solution. Therefore, the above equation can be transformed to:

$$E_{Reading} = E_{membrane} - a\ constant$$

According to the previous electrochemical theory, the voltage on the membrane depends on the ion concentration.

$$E_{membrane} \propto C[Na^+]$$

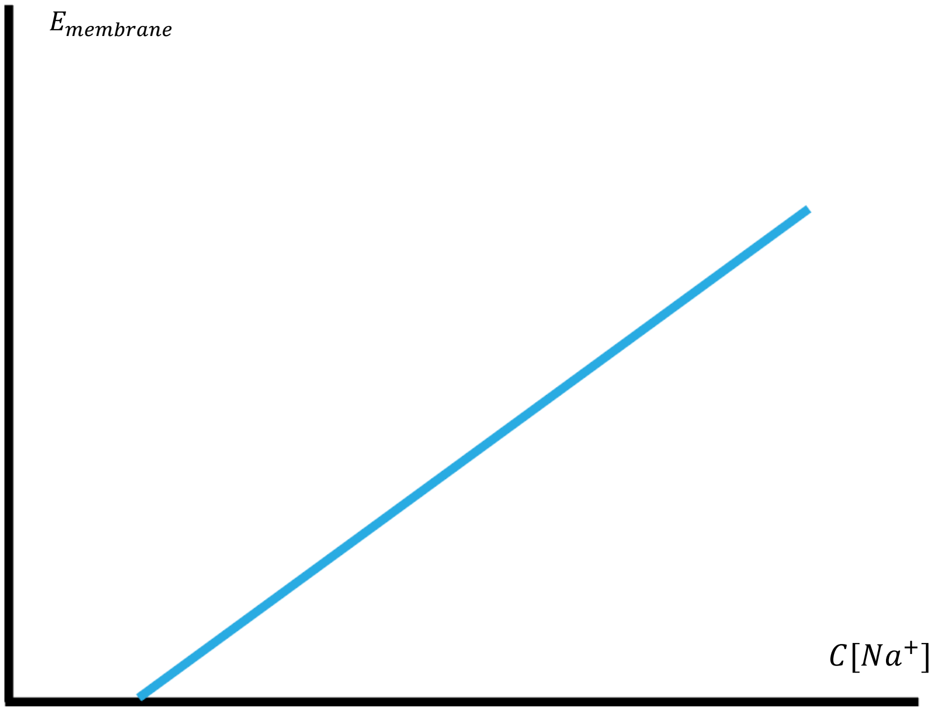

Figure 2 Responding Curve of Nernst Equation

2.2.3 Standard Electrode Potential

The standard electrode potential is to arrange the half-cell reactions according to the potential from low to high to judge the direction of the redox reaction. Usually people call the potential difference between the electric double layer between the metal and the salt solution as the electrode potential of the metal and describe the relative strength of the electrode's ability to gain and lose electrons. The electrode potential is represented by the symbol $E_{Mn\ or\ Mn^{+}}$ in V (volts). In this research project, it is the relationship between the electromotive force generated by the gain and loss of electrons in the metal salt solution and the concentration of the metal salt solution. The standard electrode potential is the potential of the reversible electrode in the standard state and the equilibrium state, that is, the electrode potential in the standard state. The aqueous solution of sodium chloride used in the research project is obtained from the dissolution of sodium chloride crystals, and there will be impurities such as chromium, cobalt and nickel in the crystals. These impurities can also generate electromotive force when dissolved in water and have an impact on the final result. How to eliminate or avoid the impact of these impurities in water is also a key problem that I need to solve in this project. The method of eliminating interference will be explained in detail when Chapter 3 introduces the electrode experiment.

Table 3 Standard Electrode Potential of common positive ions

Half-cell Reaction	Standard Electrode Potential
$Li^{+} + e^{-} = Li(solid)$	-3.09V

$K^{+}+e^{-}=K(solid)$	-2.931V
$Na^{+}+e^{-}=Na(solid)$	-2.71V
$Cr^{3+}+3e^{-}=Cr(solid)$	-0.74V
$Co^{2+}+2e^{-}=Co(solid)$	-0.28V
$Ni^{2+}+2e^{-}=Ni(solid)$	-0.25V

2.2.4 Modification of Electrodes and Various Types

As mentioned above, for the working electrode to specifically react with ions in the solution to generate a polarization potential, it must have the characteristics of being able to select such ions. The most common method is to cover the surface of the working electrode with an ion-selective membrane where generates a potential difference. A typical ion-selective membrane consists of a PVC coating, a plasticizer, and an ionophore. The PVC coating provides a base for the film, and the plasticizer makes its structure more three-dimensional and stable. Ionophores are why this membrane can react to a particular ion.[12]

Figure 7 shows three different sodium ion carriers. It can be seen from the structure that they all have a common group. This group is a closed structure. This structure can carry sodium ions and transport them effectively. There are two types of ionophores: channel-forming ionophores and ion-carrying ionophores. Obviously, as the electrode of the wearable device, an ion-carrying ionophore is used.[13] When making a modified electrode, apply the ion-selective membrane solution to the working electrode, wait for it to dry at low temperature, and the effectiveness can last up to six months. The configuration of the ion-selective membrane is to mix the liquid PVC coating, plasticizer and ionophore in proportion, which contains great variability. Different types of ionophores and the ratio of the other two substances will affect the properties and effects of the final membrane. And whether the plasticizer will affect the capacity and activity of the ionophore, after the ionophore is determined, it takes a lot of time to conduct experiments, configure the ion-selective membrane solution and perform electrochemical tests on it. Due to the limited time of this master thesis project and the topic of thesis is the “Feasibility study of wearable sweat ion sensors”, the specific ion-selective membrane will not be manufactured in this project, but a commercial modification will be purchased And then connect it to the designed and fabricated circuit.

Not only the working electrode needs modification, but sometimes the reference electrode also needs modification. The reference electrode should be Ag / AgCl, and sometimes the unmodified electrode is a carbon array covered with silver. At this time, the reference electrode needs to be modified. Compared to the complexity of the working electrode modification, the modification of the reference electrode is much simpler, and it can be done with only an external voltage source. First drop the sodium chloride solution on the reference electrode, connect the reference electrode and the working electrode to the positive and negative electrodes of the power supply respectively and give them a constant 0.5V voltage for 2 minutes. The following reactions will occur on the reference electrode:

$$Ag + NaCl \rightarrow AgCl + Na^{+}$$

Whether the reference electrode is modified can be directly observed because sterling silver is silvery shiny and silver chloride is dark.

Figure 3 Comparison of modified and unmodified reference electrode

The product of the CIT used this theory to build their own electrode, which is not only detect the ions in sweat, but the enzymatic sensors is in this array and be detected at the same time.

2.3 Signal Processing and Functional Circuit

2.3.1 Necessity of Signal Processing

The biological signals are weak and small, they are hard to measure. In this case, the signal processing is necessary and vital in whole procedure. Furthermore, noise is inevitable during the experiment.

It has been explained above that the quantitative analysis of ions or metabolites in sweat is to convert its concentration information into a voltage signal such as a potential change. However, the concentration of substances in sweat is relatively low, and the amplitude of the corresponding voltage signal is also low. In this case, the process of signal processing needs to stabilize the voltage signal within a measurable range and eliminate noise interference. In this process, the amplifier circuit and the filter circuit are the two most essential circuits.

2.3.2 Operational Amplifier Circuit

Operational amplifiers can be broadly divided into the following categories:
1. Universal operational amplifier
2. High resistance operational amplifier
3. Low-temperature drift-type operational amplifier
4. High-speed operational amplifier
5. Low-power operational amplifier
6. High-voltage and high-power operational amplifier

1. Universal operational amplifier

Its performance index can be suitable for general performance (low frequency and slow signal change), such as LM358, LM324 and field effect tube as input stage LF356.

2. High resistance operational amplifier

The characteristic of this type of op amp is that the differential mode input impedance is very high and the input bias current is very small. The main measure to achieve these indicators is to use the high input impedance characteristics of the field effect tube, but the input offset voltage of this type of op amp is relatively large. Such op amps include LF356, LF355, LF347, CA3130, etc.

3. Low-temperature drift-type operational amplifier

In automatic control instruments such as precision instruments and weak signal detection, the offset voltage of the op amp is expected to be small and not to change with temperature. The bottom temperature floating type op amp is designed for this. Typical ones are OP07, AD508, etc.

4. High-speed operational amplifier

In fast A / D and D / A and in video amplifiers, the conversion rate SR of the op amp must be high, and the unity gain bandwidth BWG must be large enough. The main features of high-speed op amps are high conversion rate and wide frequency response. Common ones include LM318.

5. Low-power operational amplifier

Due to the expansion of the application range of portable instruments, it is necessary to use low power supply voltage and low power consumption op amps. Common ones include TL-022C and TL-160C.

6. High-voltage and high-power operational amplifier

The output voltage of the op amp is mainly limited by the power supply. In ordinary op amps, the maximum value of the output voltage is generally only tens of volts, and the output current is only tens of milliamperes. To increase the multi-output voltage or output current, auxiliary circuits must be added outside the op amp. The high-voltage high-power op amp can output high voltage and large current without any additional circuit.

2.3.3 Low-pass Filter Circuit

A low-pass filter is a circuit that allows signals below the cut off frequency to pass and filters signals above the cut off frequency. Common types nowadays are Butterworth filters and Chebyshev filters. The difference is that when the filters have the same order: the Butterworth filter has the flattest passband and the stopband drops slowly; the Chebyshev filter has other ripples, and the stopband drops faster. In practical use, the Butterworth filter is more common because it can obtain more stable and flat results.[14] The active low-pass filter circuit consists of an integrated op amp and passive component resistors and capacitors. It can pass a signal from zero to a certain cut off frequency without attenuation. Its design also depends on the modification of the op amp circuit. It can effectively eliminate high-frequency interference signals. When designing an active low-pass filter, the op amp circuit also requires high input impedance and low output impedance, and the open-loop gain must be sufficiently large. In this case, the cut off frequency:

$$f_c = \frac{1}{2\pi R_2 C}$$

The gain is $-\frac{R_2}{R_1}$.

The order of the filter is the order of filtering the harmonics. For the selection of the filter order, generally, the higher the order, the better the filtering effect, but the corresponding cost will be higher, so the actual order of the filter should be determined based on the actual project.

Chapter 3 Electrodes Principle

The first part of my research project is to select suitable electrodes to collect sodium ion concentration information in the solution. In this part, I used three different types of electrodes to measure the sodium ion concentration in a multi-concentration sodium chloride aqueous solution. In this chapter, I will introduce these three different types of electrodes including their working principle and experimental process. And the results of the three electrodes and their respective advantages and disadvantages will be elaborated in Chapter Results. In addition, the first part of my research is based on the AUTOLAB electrochemical workstation.

3.1 Three-electrode System of Saturated Calomel Electrode

As described in Chapter 2, the electrode part of the electrochemical system initially used a three-electrode system with a saturated calomel electrode as the reference electrode. In this three-electrode system, the saturated calomel electrode is the reference electrode, the platinum plate electrode is used as the working electrode, and the carbon rod electrode is used as the counter electrode.

3.1.1 Principle of Saturated Calomel Electrode

The saturated calomel electrode uses a high concentration of potassium chloride solution as the electrolyte, and the concentration of potassium chloride reaches 4.2 mol / L. In the standard state, the electromotive force of the saturated calomel electrode at 25 ° C is 0.2412V and remains unchanged. This feature can be used as a salt bridge, or as a reference electrode for aqueous electrochemistry.

Reaction of the SCE potential:

$$Hg_2Cl_2 + 2e^- \leftrightarrows 2Hg + 2Cl^-$$

$$E^0_{Hg_2Cl_2\backslash Hg_2Cl^-} = +0.27V$$

$$E_{\frac{1}{2}SCE} = E^0_{Hg_2Cl_2\backslash Hg_2Cl^-} - \frac{RF}{2F} ln a^2_{Cl^-}$$

As expressed by the above formula, when the saturated calomel electrode is used as the reference electrode, the only variable affecting its electromotive force is the concentration of chloride ions in the solution. However, the interior of the electrode has been saturated with potassium chloride solution, and the concentration chloride in the electrode is unchanged, the electromotive force generated on the electrode will not change.

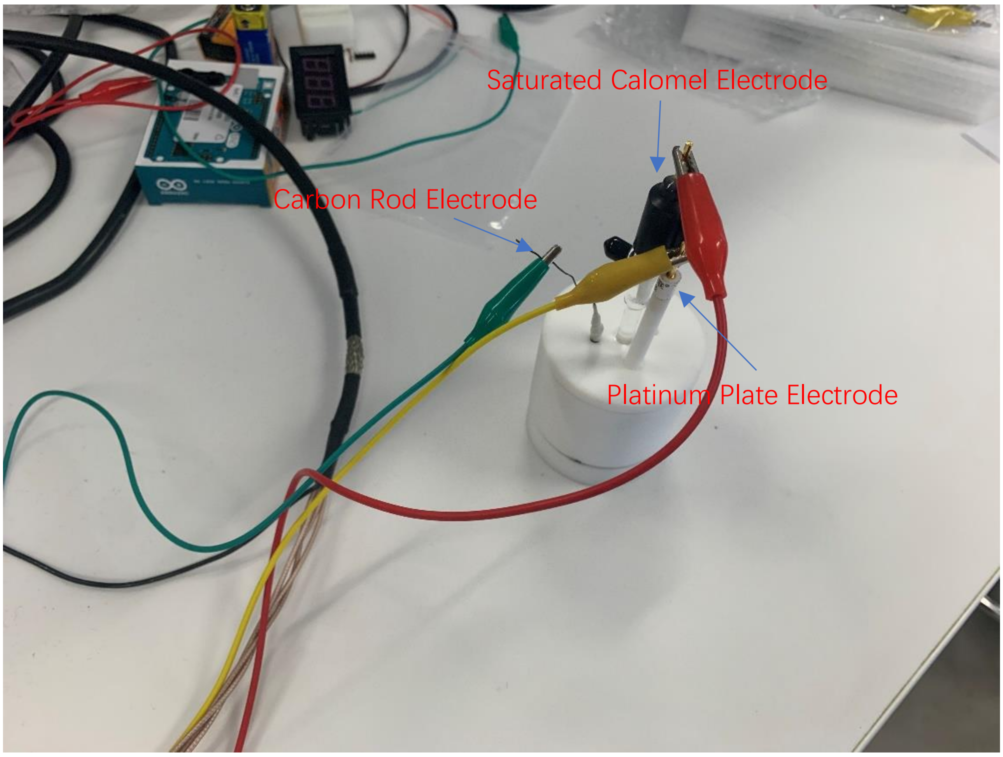

Figure 4 Three Electrode System of SCE

3.1.2 Elimination of Interference

As I introduced earlier, the sodium chloride aqueous solution used in the experiment was obtained by directly dissolving sodium chloride crystals. During this process, compound crystals of chromium, cobalt and nickel will be doped in the sodium chloride crystals and dissolved together in water. In this case, there are positive chromium ions, cobalt ions and nickel ions in the solution. The redox reaction in the solution will also release the electromotive force, which will affect the final results of my research project. In the saturated calomel electrode system, the sedimentation method is used to remove the interference of impurity cations in the solution.

There are two steps to reduce the impurity.

The first step is to stay the electrochemistry system for a while (10 minutes), wait the reduction action and the result reliable relatively.

The second step is to use a sacrifice electrode to eliminate the impact. The specific approach is using a material with superhigh conductivity like carbon or copper as the working electrode gets into the circuit, and use the function of ‘i-t curve’ in the AUTOLAB, give a constant voltage (-2 V) and 10 seconds. The given voltage must be higher than the standard electrode potential of the impurities. It can make the positive ion sediments on the sacrifice electrode. And the result is a pure NaCl solution.

The choice of -2V as the reaction voltage is based on the standard electrode potential of different cations. The standard electrode potential of sodium ions is -2.71V, which means that when the amplitude of the external electromotive force is higher than this value, the sodium ions in the solution will undergo a reduction reaction, and the ions become solid sodium. The standard electrode potentials of the impurity ions chromium, cobalt and nickel are far below this amplitude. Therefore, when a voltage of -2V is applied to the solution, only the impurity ions will undergo a reduction reaction, thereby achieving the purpose of removing impurities.

However, the content of impurity ions is very rare, and the diluted crystals are difficult to be found by the naked eye. The results of this part will be shown in detail in the Chapter Results of the AUTOLAB experiment on saturated calomel electrodes.

3.2 Two-electrode System of Screen-printed Electrode

The second step in this part of my research project was to use commercial screen-printed electrodes. Unlike the saturated calomel electrode, the screen-printed electrode (SPE) has the characteristics of flexibility and small size. And it is also a three-electrode system, with working electrode, reference electrode and counter electrode. However, considering that only the potential parameters in the electrode system are used, I only connected the working electrode and the reference electrode, but not the counter electrode.

3.2.1 Principle of Screen-printed Electrode

The screen-printed electrode uses pure silver as the working electrode and silver chloride as the reference electrode. The electrode potential of the silver chloride electrode can be derived from the electrode potential of the silver electrode:

Silver electrode:

$$Ag^{+} + e^{-} \rightarrow Ag$$

Nernst Equation:

$$E = E_0\left(\frac{Ag^{+}}{Ag}\right) + 0.05916\log\,[Ag^{+}]$$

Add Cl^{-} on both sides of the silver electrode reaction equation:

$$Cl^{-} + Ag^{+} + e^{-} \rightarrow Ag + Cl^{-}$$

That is:

$$AgCl + e^{-} \rightarrow Ag + Cl^{-}$$

Nernst Equation:

$$E = E_0\left(\frac{AgCl}{Ag}\right) + 0.05916\log\left[\frac{Ag^{+}Cl^{-}}{Cl^{-}}\right] = E_0\left(\frac{AgCl}{Ag}\right) + 0.05916\log(Ksp[Cl^{-}])$$

$$= E_0\left(\frac{AgCl}{Ag}\right) + 0.05916\log[Cl^{-}]$$

To detect the concentration of the sodium, it needs a two-electrode system instead of a three-electrode system.

For the connection, the working electrode is connected with the support electrode, and the reference electrode is connected with the counter electrode.

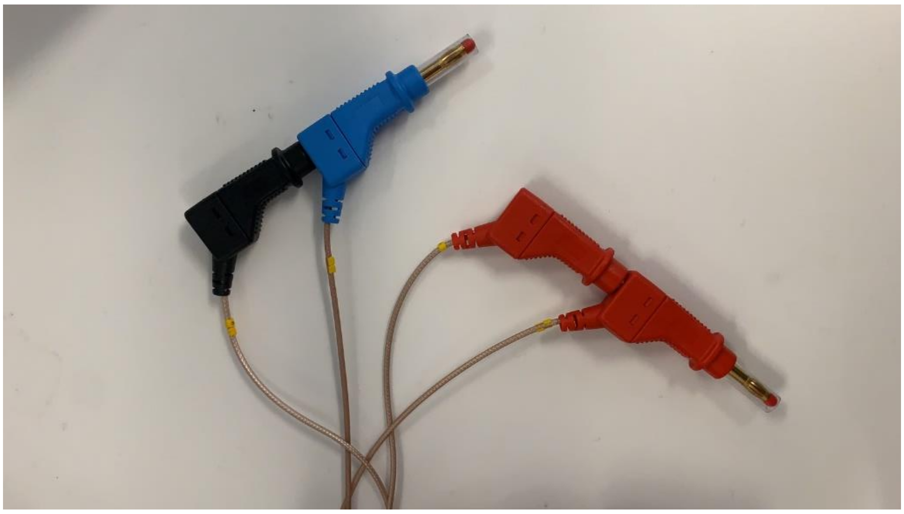

Figure 5 Connector of Two-Electrode System

A series of results were obtained at different concentrations by connecting screen-printed electrodes with AUTOLAB electrochemical workstation. These results are also not discussed in this chapter, and are discussed in detail in Chapter Result.

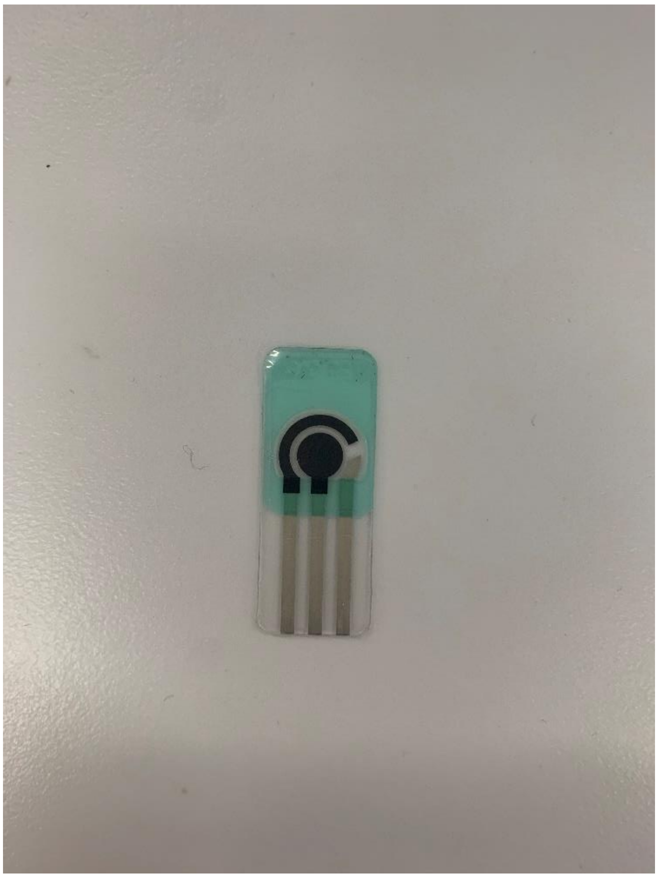

Figure 6 Screen-printed Electrode

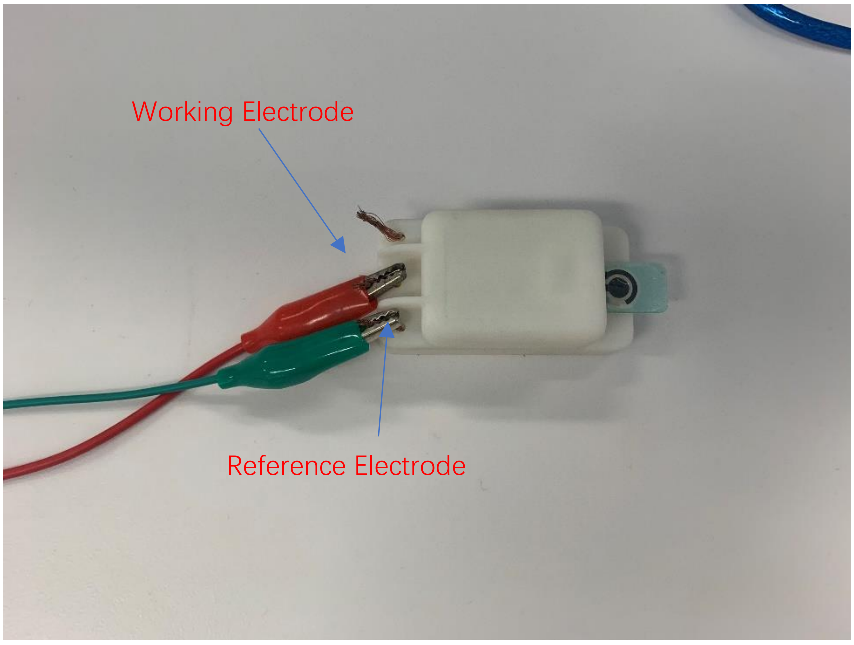

Figure 7 Two-Electrodes System of SPE

3.2.2 Modifying of Reference Electrode

It needs to be clarified that silver chloride is used as the reference electrode because the pure silver is active. And the pure silver is bright and silver chloride is dark. The initial screen-printed electrode was that all electrodes were pure silver electrodes, not the silver chloride electrodes described. For this reason, in order to meet the needs of research, I said that the reference electrode of each electrode was modified into a silver chloride electrode.

In order to convert pure silver to silver chloride, I used Ag as the working electrode and continued it at a constant voltage of 1V for 2 minutes. At this time, the following reactions will occur on the electrode:

$$Ag + NaCl \rightarrow AgCl + Na^{+}$$

The modified reference electrode becomes a silver chloride electrode, which conforms to the silver / silver chloride electrochemical system. In order to prove the stability of the obtained silver chloride electrode, I also connected it as a working electrode on an AUTOLAB electrochemical workstation, and then measured its potential in different concentrations of sodium chloride solution, obtained a series of results, these results will also be analysed in Chapter Result.

3.3 Two-electrode System of Modified Screen-printed Electrode

The last part of the electrode part of my research project is to use a modified screen-printed electrode to connect to the AUTOLAB electrochemical workstation. Similar to the previous experiment with screen-printed electrodes, I also used only a two-electrode system that only connected the working electrode and the reference electrode.

3.3.1 Principle of Modified Screen-printed Electrode

Same as the screen-printed electrode made in the previous section, this electrode is also a silver / silver chloride electrode. Because the aqueous solution of sodium chloride used is a neutral solution, a silver chloride electrode is more suitable. The interior of the saturated calomel electrode is a potassium chloride solution, which is a strong acid and alkali salt. The potential is stable but it is easily affected by temperature and the temperature lag is obvious. The silver chloride electrode is not only easy to prepare, stable potential, good reproducibility, but also the electrode structure is firm, the temperature lag is small, and when the temperature changes, it can quickly reach the equilibrium potential at the new temperature, and can be used at high temperature.

But unlike the previous screen-printed electrode, the working electrode part of this electrode is modified. The working electrode indicates that there is a layer of sodium ionophore, which will specifically combine with sodium ions to form a polymer and isolate its charge from the surrounding environment. Sodium ions cross this layer of membrane, while other cations cannot cross the selective membrane. In this case, only sodium ions are undergoing a reduction reaction on the working electrode, and the potential detected by the working electrode is only the potential released by the reduction reaction of sodium ions.

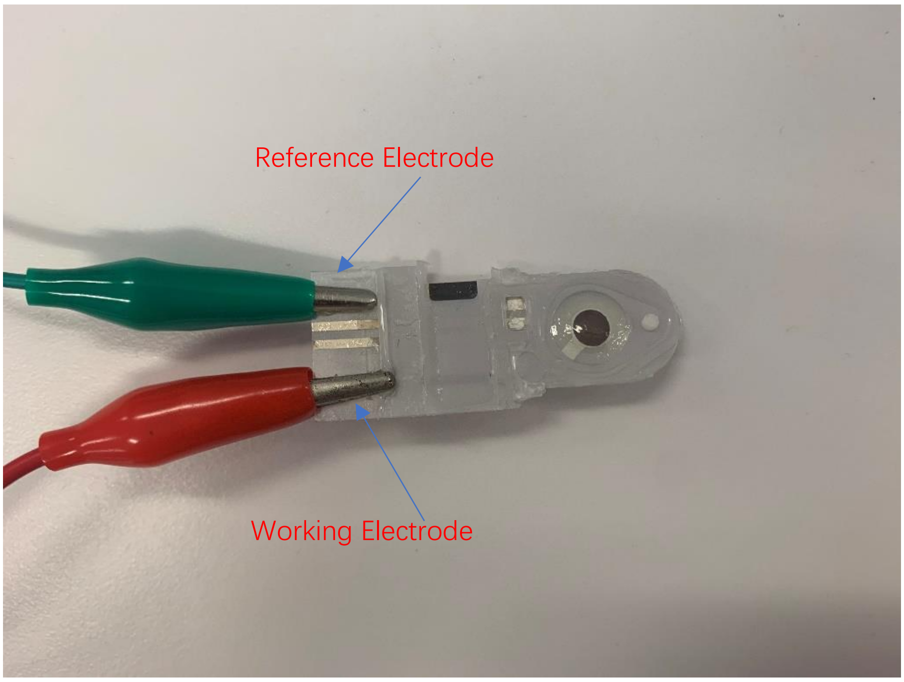

Figure 8 Two-Electrode System of Modified SPE

It can be seen from the figure above that the reference electrode of this electrode is dark silver chloride, indicating that it has been modified. The other counter electrode and support electrode do not need to be connected to the circuit.

Chapter 4 Circuits Design

In this chapter, I introduce the second part of my research, the proc of processing the electrochemical potential signal obtained in the previous part. In order to realize signal collection and processing, I designed a series of circuits to process the obtained signals, including inverter, amplifier and filter circuits. This chapter mainly introduces the design process and also contains some basic principles of components and circuits.

4.1 Reasons for choosing the LT1462

The amplifier I used is the LT1462 integrated op amp. It has a total of 8 pins, including two input ports and two output ports. And it can provide micro-amp operational amplifier with micro-ampere input bias current and unity gain stability.[15] This characteristic makes it suitable for situations where the input and output impedances are in a wide range, increasing the flexibility of circuit design. For my research project, because all I get is millivolt-level electric potential, its frequency and amplitude are very small, so it is very suitable to choose LT1462.

In addition, LT1462 is suitable for photocurrent amplifier, low frequency micropower active filter, because my circuit contains both amplifier circuit and filter circuit, choose the same type of integrated op amp, power supply can be used in one source.

Furthermore, I am designing a wearable sensor device, in this case, the smaller the circuit, the better. These two input and output ports can be used at the same time to reduce the size of the circuit board when making hardware in the future. The specific content will be described in detail in Chapter 5 later.

In addition to the above-mentioned functional reasons, economy is also an advantage. Its price is cheaper than similar products, each is about 6 Australian dollars. Because my research will cost a lot of components, so the low price is why I chose it.

4.2 Design of Voltage Buffer Circuit

For the buffer amplifier circuit, I use an inverse closed-loop amplifier circuit, which connects a $1M\Omega$ resistor negative feedback to the amplifier. In this case, part of the output voltage will be applied to the reverse input terminal to achieve negative feedback, reducing the amplifier. Total gain, which is the gain of the circuit is determined by the resistance in the feedback network.

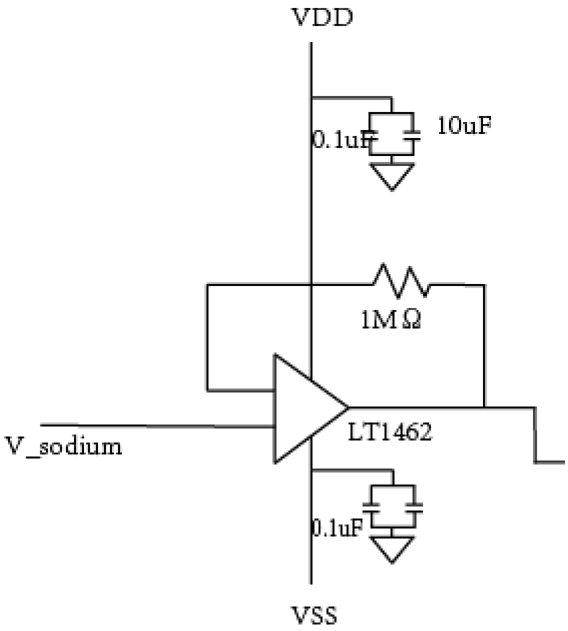

Figure 9 Voltage Buffer Circuit

In addition, this part of the circuit also plays the role of collecting the potential signal of the sodium ion electrode and the potential signal of the reference electrode at the same time.

It consists of two identical voltage buffer circuits, and then sends these two signals to the next circuit (amplifier circuit) for processing. The structure of the circuit is exactly the same, which means that the function is also the same. It is to make the collected signal not directly affected by the amplifier and directly pass into the next functional circuit.

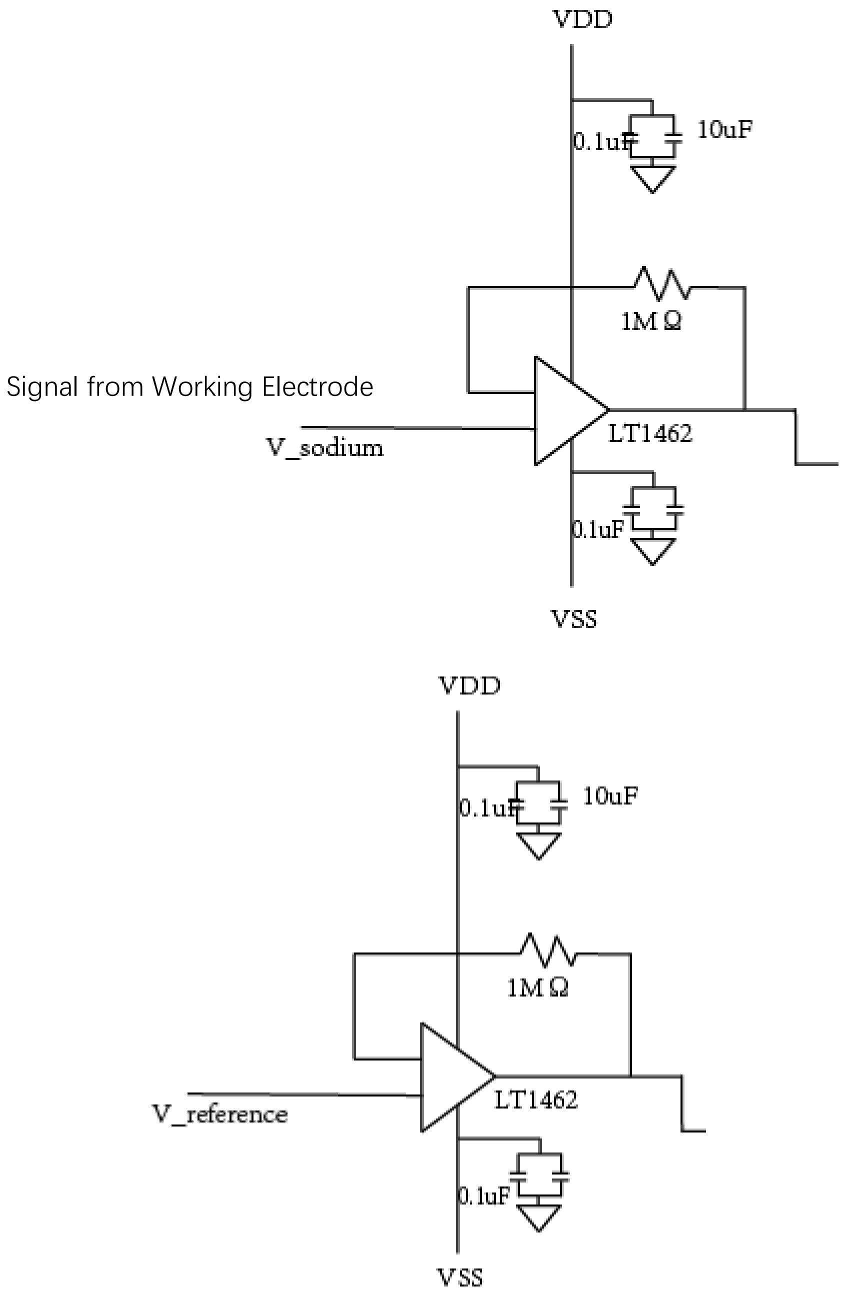

Figure 10 Voltage Buffer Circuit for Two Inputs

4.3 Design of Differential Amplifier

After the voltage buffer circuit, I designed a differential amplifier circuit to further process the collected signal. Because two voltage signals are collected, and through knowledge of electrochemistry, the open circuit potential what we need is the potential on the working electrode minus the potential on the reference electrode. Therefore, we need to design a subtractor.

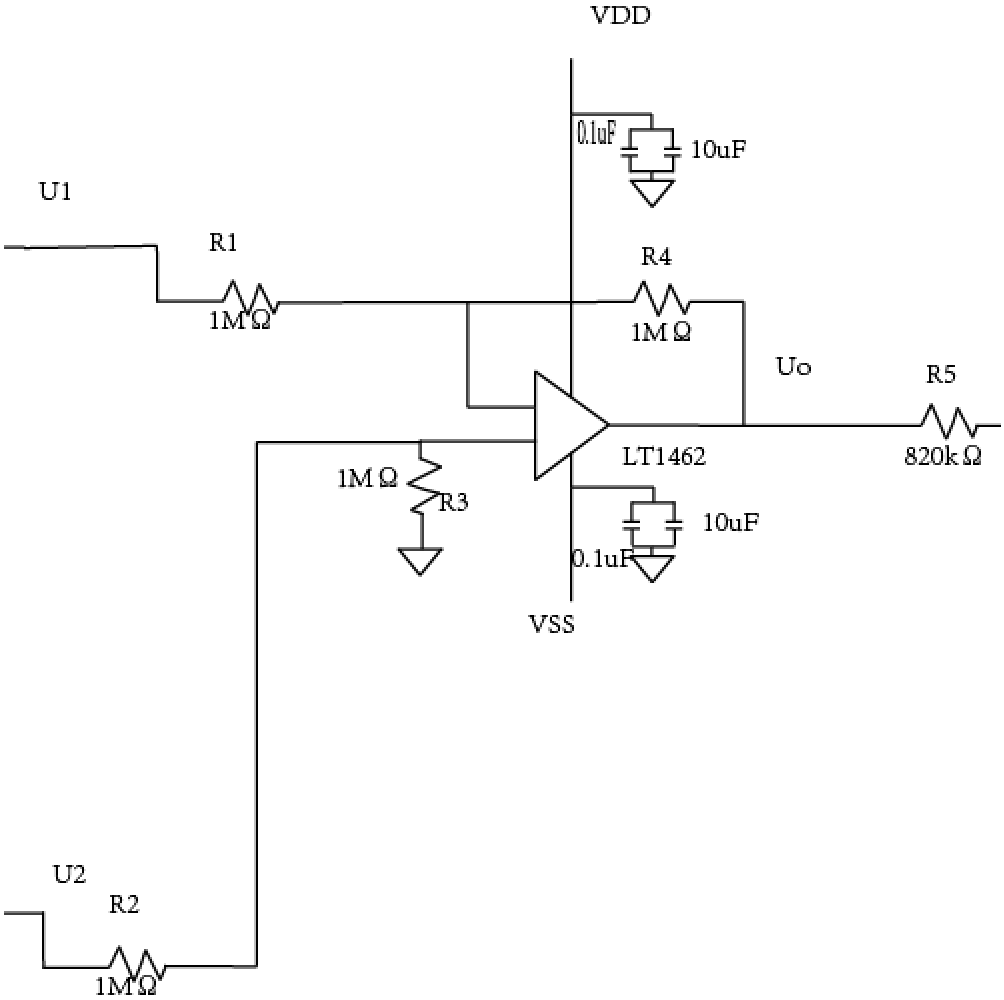

Figure 11 Differential Amplifier

As shown in the picture is the subtractor I designed, it is a typical differential amplifier circuit. The formula for calculating its output voltage is:

$$U_O = \frac{(R_2 + R_4) * R_3 * U_1}{(R_1 + R_4) * R2} - \frac{R_4 * U_2}{R_2}$$

And $R_1 = R_2 = R_3 = R_4 = 1M\Omega$

$$U_O = U_1 - U_2$$

In addition, it is also a reverse closed-loop amplifier, which can amplify and invert the result calculated by the subtractor, and then output it to the filter circuit of the next stage.

The amplification gain of this circuit is not very large, because I am worried that increasing the gain of the amplifier will necessarily increase the resistance of the output terminal. If the resistance of the output terminal is too large, the voltage at the output terminal will increase, which may affect the normal operation of the op amp may even destroy the op amp.

4.4 Design of 4th Butterworth Filter

After the above circuits are designed, a filter is needed to filter the signal. In fact, I put two capacitors in parallel on each section of the circuit to perform a preliminary filtering.

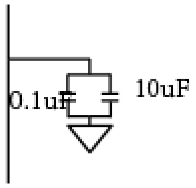

Figure 12 Primary Filter Circuit

The large-capacitance capacitor is for the existence of filtering, while the small-capacitance capacitor is to eliminate the interference of high-frequency signals.

For the fourth-order low-pass Butterworth filter circuit, the combination of high impedance and low capacitance is the condition of my design circuit. The characteristic of Butterworth filter is that the frequency response curve in the pass band is as flat as possible, without fluctuations, and gradually decreases to zero in the stop band. On the Bode diagram of the logarithmic diagonal frequency of the amplitude, starting from a certain boundary angular frequency, the amplitude gradually decreases with the increase of the angular frequency and tends to negative infinity.[16]

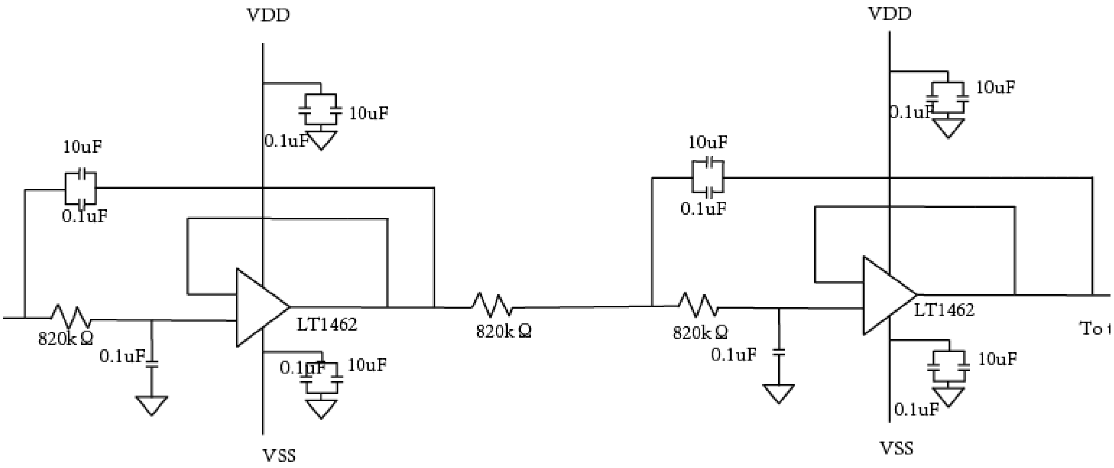

Figure 13 4th Butterworth Low-pass Filter Circuit

The square amplitude response of the Butterworth low-pass filter is:

$$|H(jw)|^2 = \frac{1}{1 + \left(\frac{\omega}{\omega_c}\right)^{2\pi}}$$

The fourth-order active low-pass filter I used is composed of two cascades of two second-order low-pass filters. Its transfer function is:

$$G_4(s_\lambda) = \frac{G_{01}}{s_\lambda^2 + \xi_1 s_\lambda + 1} * \frac{G_{02}}{s_\lambda^2 + \xi_2 s_\lambda + 1}$$

In order to meet the above conditions,

$$C_1 = C_2, R_1 = R_2$$

The production of a fourth-order Butterworth filter can be completed by ensuring that the corresponding resistance and capacitance values of the first and second stages are the same.

The damping coefficients of the two second-order Butterworth filters are:

$$\xi_1 = 0.765$$

$$\xi_2 = 1.848$$

Hence, the two zero-frequency gains are:

$$G_{01} = 3 - \xi_1 = 3 - 0.765 = 2.235$$

$$G_{02} = 3 - \xi_2 = 3 - 1.848 = 1.152$$

The transfer function:

$$G_4(s_\lambda) = \frac{G_{01}}{s_\lambda^2 + \xi_1 s_\lambda + 1} * \frac{G_{02}}{s_\lambda^2 + \xi_2 s_\lambda + 1} = \frac{2.235}{s_\lambda^2 + 0.765 s_\lambda + 1} * \frac{1.152}{s_\lambda^2 + 1.848 s_\lambda + 1}$$

At this point, the circuit design has been completed. In the next chapter, the process of simulating the circuit after completing the circuit design will be introduced.

Chapter 5 Simulation of Function Circuit

In this chapter, the process of simulating these circuits after designing the functional circuits that process the electrochemical signals received by the electrodes is introduced. What is introduced in this chapter is only the process of simulation and the operation of signal input. The results of the specific simulation will still appear in Chapter Results to elaborate.

5.1 Build of Function Circuit in NI MultiSIM 14

In the process of simulating the designed circuit, I used the software NI MultiSIM 14, which can perform real-time simulation and functional test on the designed circuit.

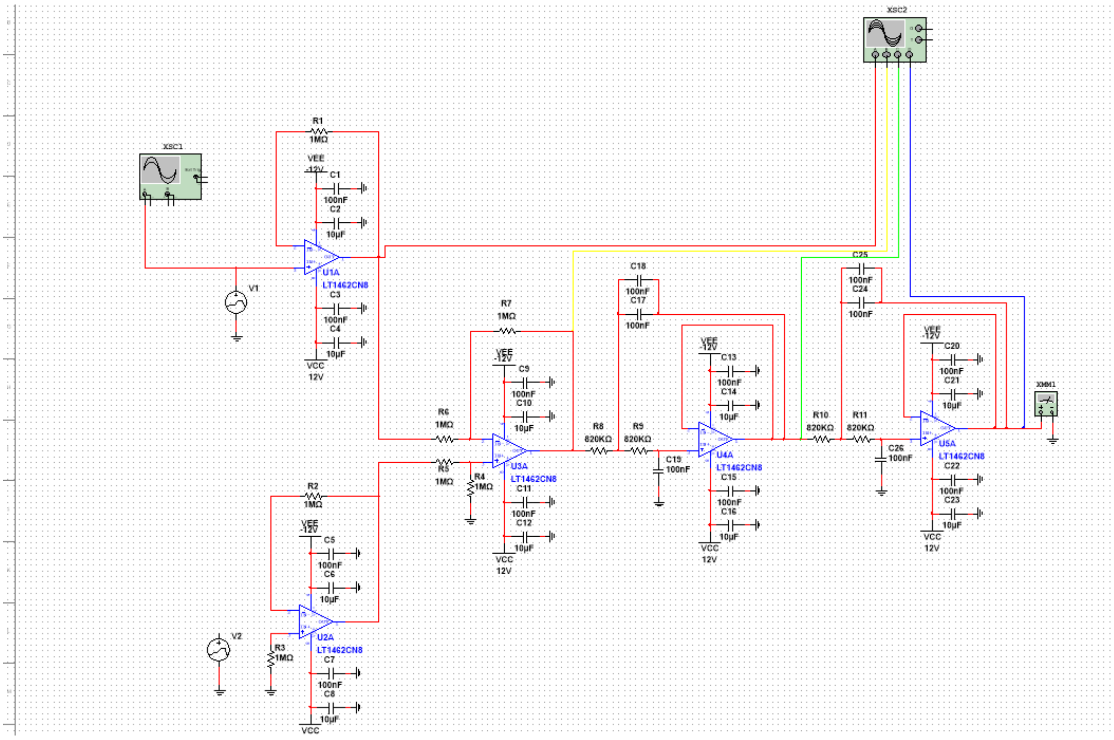

Figure 14 Function Circuit in NI MultiSIM

After completing the circuit prototype in the figure above, as long as the data is imported, the waveform change can be observed on the oscilloscope, before and after the circuit.

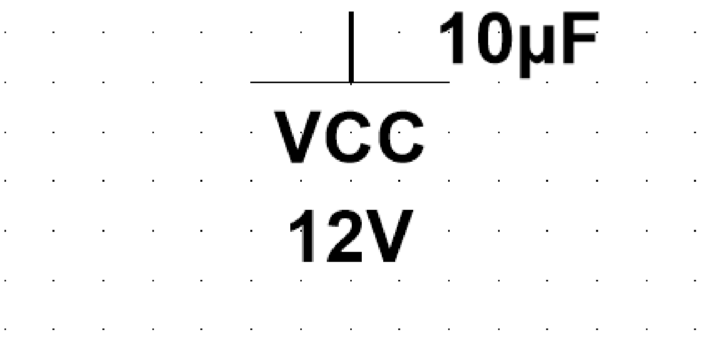

Figure 15 Power Supply

According to the LT1462 datasheet, the operating voltage of the op amp is between 10V and 20V, so I used a 12V voltage to power the op amp.

As for the prototype of LT1462, there are directly selectable components in the database.

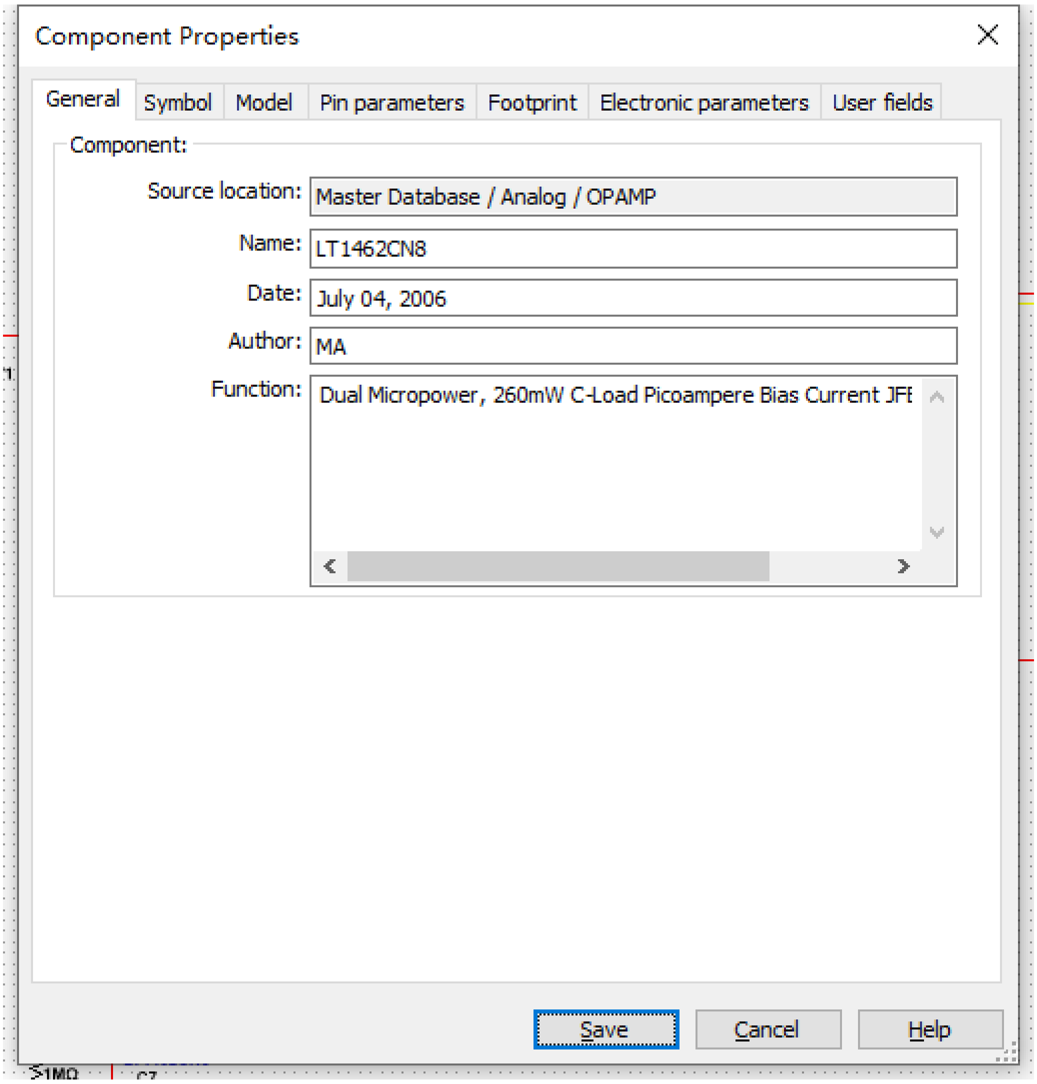

Source location: Master Database / Analog / OPAMP
Name: LT1462CN8
Date: July 04, 2006
Author: MA
Function: Dual Micropower, 260mW C-Load Picoampere Bias Current JFE

Figure 16 Information of LT1462

Therefore, the production of functional circuits in the software is not very difficult work, but how to import electrical signals collected by similar electrodes and voltage signals that change with time is a difficult problem to solve.

5.2 Source Signal File Import

The challenge in this part is how to convert the analog signal received by the electrode into an input signal and import it into this analog circuit.

During the first step of my research, the electrode was connected to the AUTOLAB electrochemical workstation, and the curve of the relationship between open circuit potential and time was obtained directly on its corresponding software NOVA 2.0. This data can be exported as a text document. I will use the third step of Part One, using the open-circuit potential source data obtained by modified screen printing as the input signal source. However, such text files cannot be directly imported into analog circuits in NI MultiSIM.

The solution is to introduce a "Piecewise linear voltage source" (PWL voltage). It allows the import of linearly varying voltage data, which can be customized for editing or imported from documents.

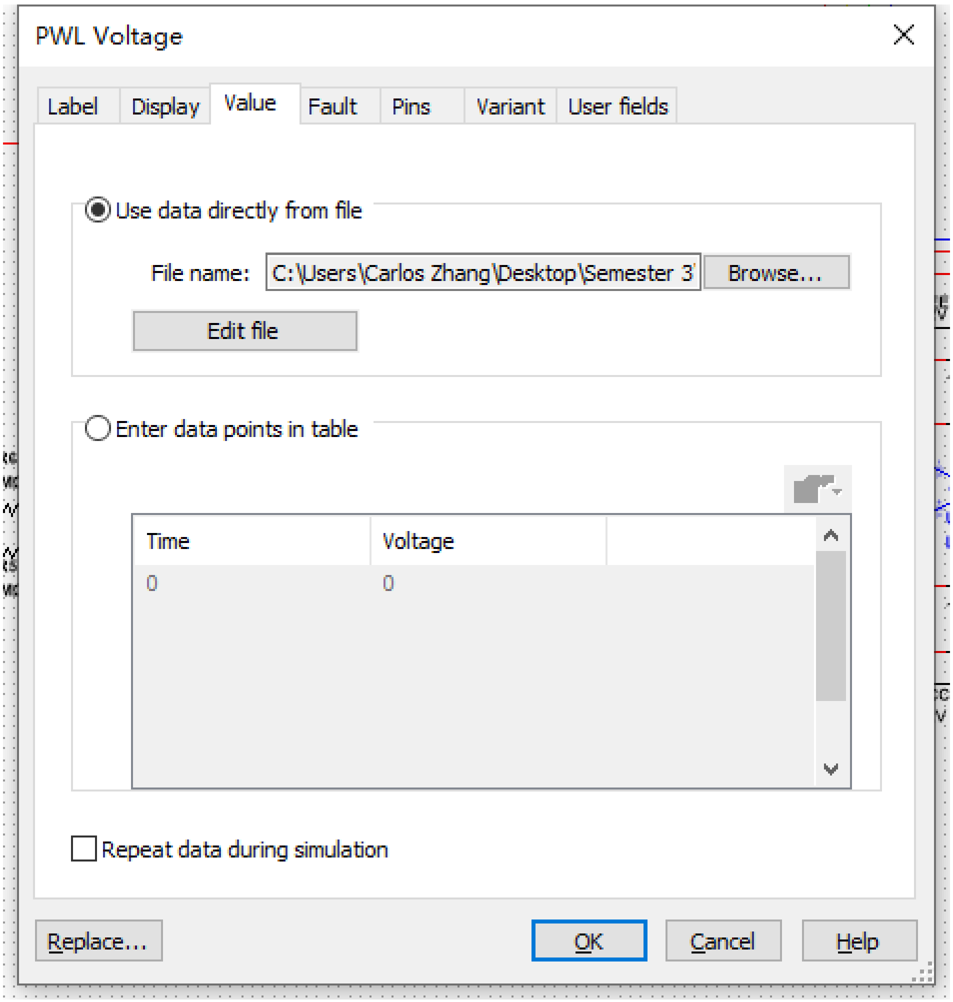

● Use data directly from file

File name: C:\Users\Carlos Zhang\Desktop\Semester 3

○ Enter data points in table

Time	Voltage
0	0

☐ Repeat data during simulation

Figure 17 Import with PWL Voltage

I will use the data of the relationship of "potential-time" obtained by AUTOLAB as the input signal and observe whether the function of this functional circuit in the simulated situation can meet the expectations. The results of this part will also be elaborated in Chapter Results.

Chapter 6 PCB Printed Circuit Board Fabrication and Assembled Device Testing

This chapter is mainly to undertake the work of the previous chapter. After the simulation on the software is completed, the hardware production is required. The original design of the subject is to make the circuit into a flexible substrate so as to be more suitable for fitting on human skin. The circuit I originally designed was not intended to be made with a traditional PCB, but a Dimatix printer was used to print the path of the circuit on a soft material substrate, and nano-silver was used as the printing ink because silver has ultra-high conductivity. The base material can be thermoplastic polyurethane (TPU), which is a highly plastic elastomer.

The original research was based on the laboratory of La Trobe University. They have the technology of using Dimatix to print circuits or sensors. However, because of the current force majeure, the laboratory of La Trobe University is closed, so I can only use the most common method using Altium Designer to draw the PCB and then make the board.

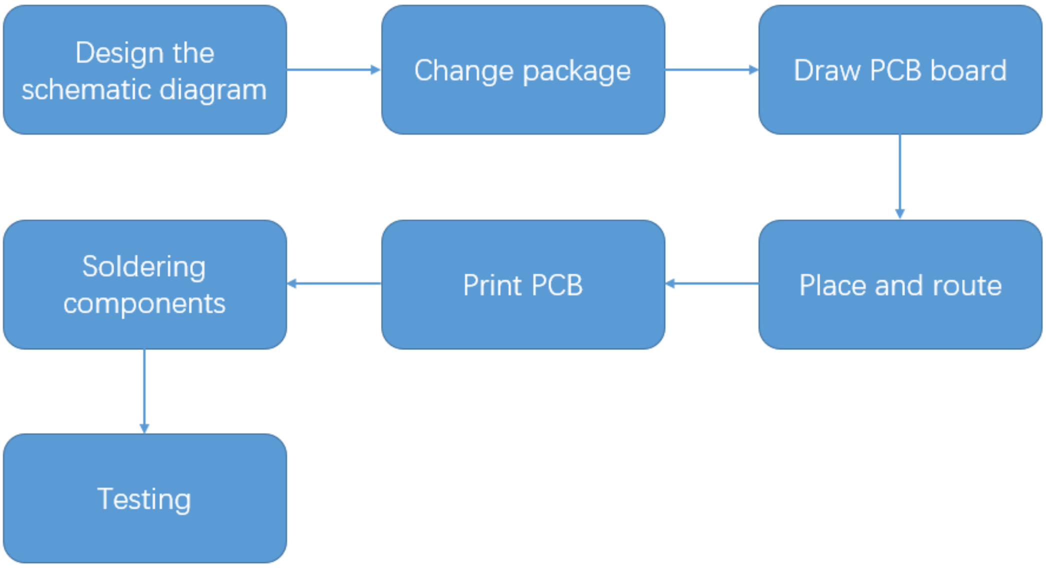

Figure 18 Procedure of Building PCB

6.1 Design the Schematic Diagram

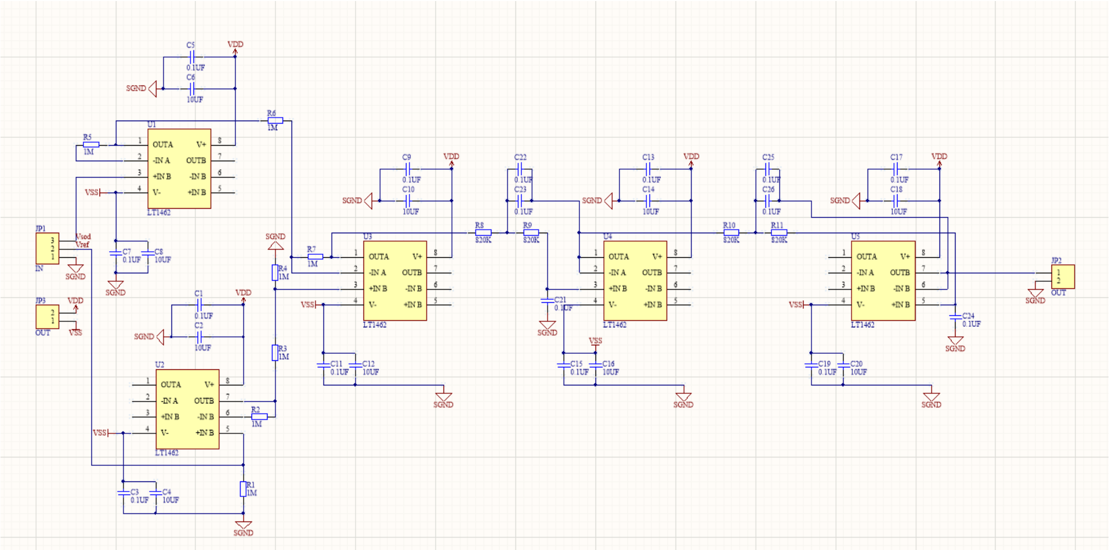

Figure 19 Schematic Diagram of 5 pieces LT1462

The picture above is the first version schematic I designed in Altium Designer. It can be seen that its design is exactly the same as the designed circuit diagram. It uses 5 LT1462 op amps. The arrangement of each component is exactly the same as the circuit at the time of design. The input end has the potential signal of the working electrode and the potential signal of the reference electrode input at the same time, so I used dual input ports. Because the output has only one open circuit potential signal through the subtractor, I only used one output port. Coupled with the reserved power interface, the circuit schematic is complete.

However, considering that the designed circuit is for wearable devices, such a design will make the circuit board very large, and it is not a flexible and foldable substrate, but the most common material: the hard fiberglass cloth base and copper wire which does not have the ability to bend. And I introduced before that the LT1462 op amp which I used has two input and output pins. And from the previous schematic diagram, it can be intuitively found that many LT1462 pins are not connected, which means that certain inputs and outputs can be connected to the same LT1462 without causing interference, which can greatly reduce the volume of the circuit board.

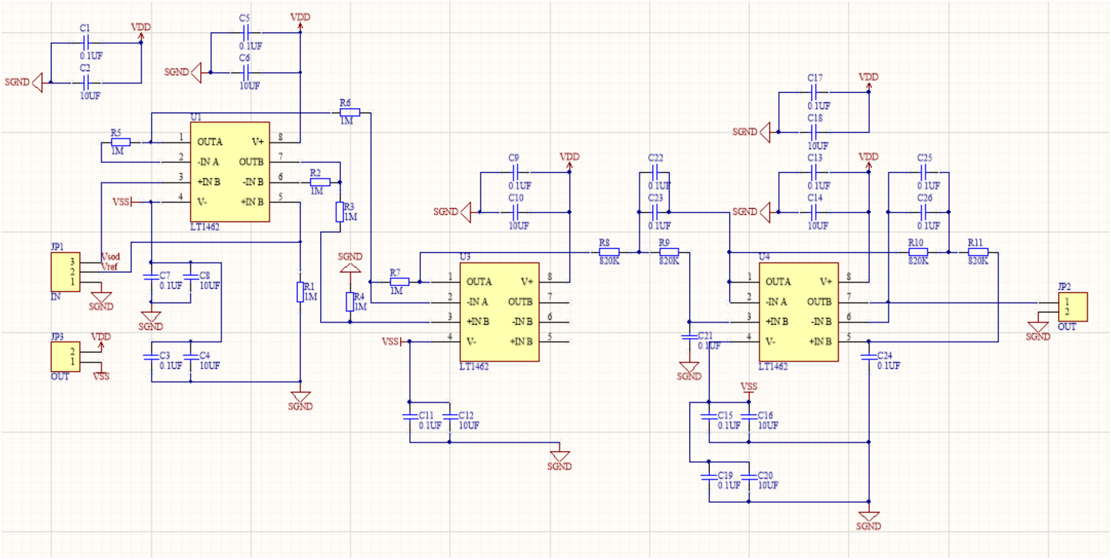

Figure 20 Schematic Diagram of 3 pieces LT1462

The figure above shows the simplified schematic, using only three LT1462 op amps. The method to achieve is to combine the two electrodes input voltage buffer circuits into one. The subtractor differential amplifier circuit uses one, and the two second-order filters combined with the fourth-order Butterworth filter use one LT1462. This design can greatly save space and can use the smallest volume to realize the function when making the board.

6.2 Building of PCB

After completing the production of the above schematic diagram, the next step is to convert the drawn schematic diagram into a PCB diagram. First select the package for all components. After the package is completed, conduct electrical inspection. After checking the correctness, create a new PCB project in the project, and then directly compile the PCB package diagram into the PCB project, and upload the previous schematic diagram in the PCB project. Place the components in the PCB board area, adjust the position of the components so that they do not overlap each other when routing. The PCB drawing is completed.

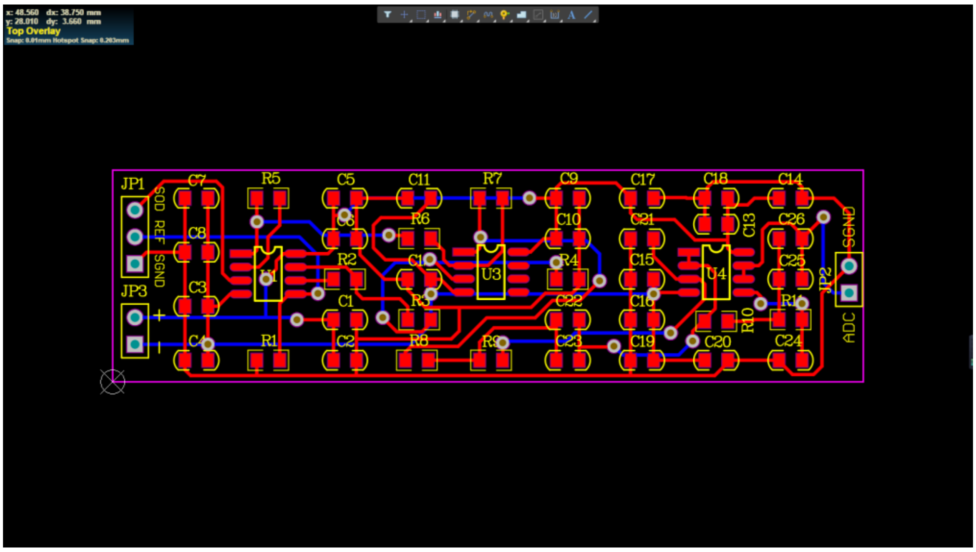

Figure 21 PCB Diagram

The size of the final PCB design is 71mm × 20mm, and the area is 14.20cm². This size is enough to be placed in a case designed as a wearable device.

After completing the PCB drawing, it can be printed directly, but our school does not have the equipment to print the PCB. The completion of this part of the project is thanks to the Engineering Service engineers at the Tonsley campus. They helped me contact the manufacturer to print the hardware circuit board and trained me on soldering components. With their help, I completed the soldering of the circuit board. The chip resistors and capacitors used and the LT1462 were soldered to the circuit board.

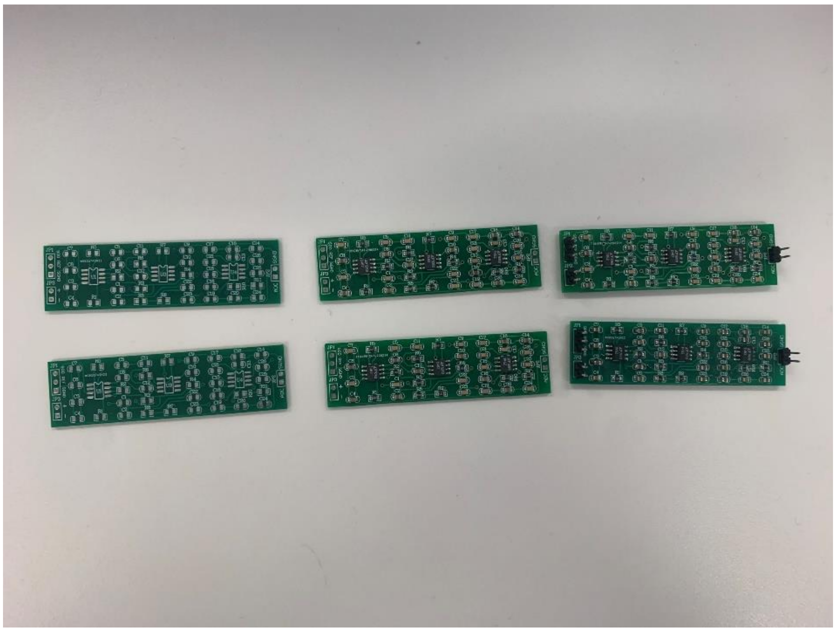

Figure 22 Soldered PCB

The picture above shows the soldered circuit board and the unsoldered circuit board.

6.3 Assembling the Device

After making the hardware of the circuit, it need to be connected to the electrodes. In this step, the display module has not been designed. In order to observe the output results, an oscilloscope in the laboratory is used. Connect the oscilloscope to observe the open circuit potential of the output.

In addition, the LT1462 needs a stable operating voltage of 10V to work properly. In order to achieve a stable operating voltage, I use the Arduino LM2596 Power Step-Down Voltage Regulator Module Voltmeter Display to complete the dry battery voltage supply.

It can use a battery to provide a stable 10V operating voltage for the device.

Its working principle is to use the op amp to increase the voltage to the required amplitude. In the process of the battery's output voltage continuously decreasing, use an inductor to resist this current change. When Q1 is activated, a larger current begins to flow via L1 to GND. When Q1 is turned off, the current flowing through L1 remains unchanged, thereby increasing the output voltage.

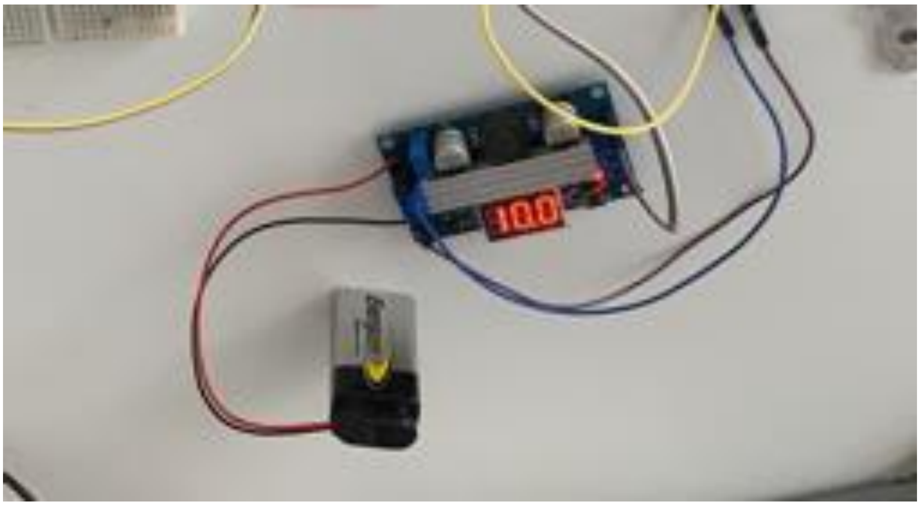

Figure 23 Power Supply of 10V

As shown in the figure above, a battery provides a stable 10V power supply for the circuit. Connect the modified screen-printed electrodes to the circuit, and then connect the output to the oscilloscope, you can visually observe the output results.

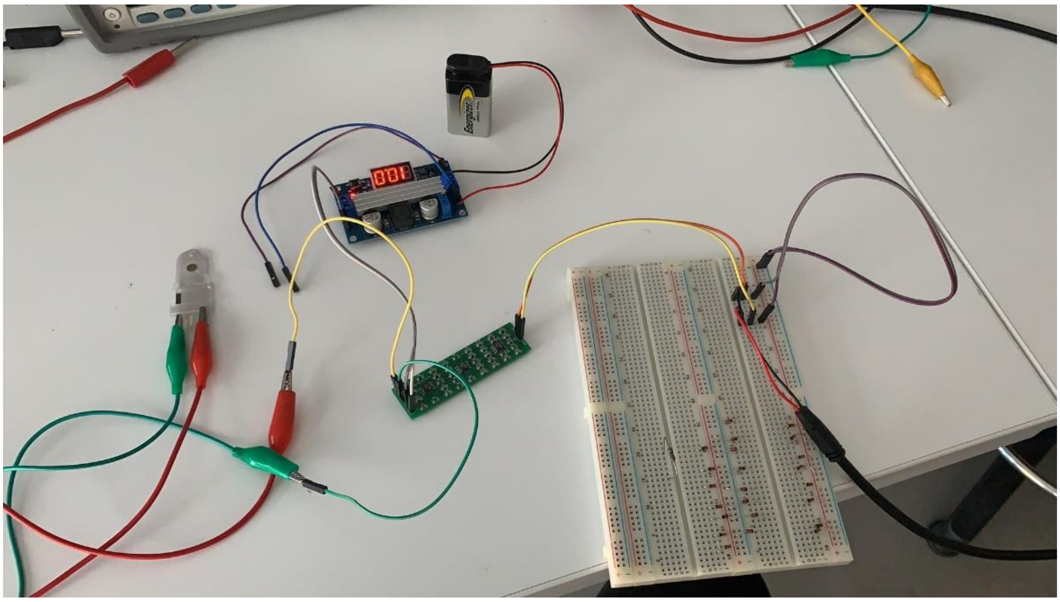

Figure 24 Connection of Electrode and Circuits

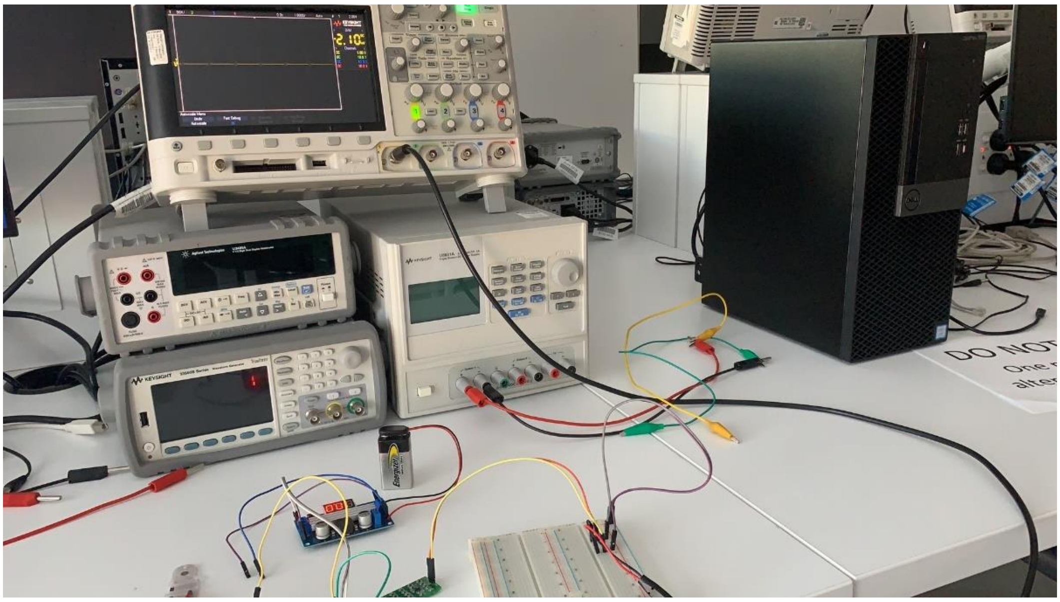

Figure 25 Connection with Oscilloscope

This chapter does not introduce the results in detail, the specific results will be explained in detail in Chapter Results.

Chapter 7 Arduino Microcomputer and LED Display

This chapter introduces that after completing the assembled device, instead of using the laboratory oscilloscope, the display module is used to display the final numbers result. I tried to connect an LED display module directly before using the Arduino MCU, and found that it could not be turned on. The reason for the analysis is that the output current is too small, only a few hundred microampere, too low current cannot make the LED display module work. Therefore, the Arduino microcomputer was used to drive an LED display module to display the voltage figures through the program.

7.1 Arduino Microcomputer

Arduino is a convenient and flexible open source electronic prototype platform. It has a Processing / Wiring development environment similar to Java and C language. There are two main parts: the hardware part is an Arduino circuit board that can be used for circuit connection; the other is the Arduino IDE, a program development environment in the computer. As long as I write the program code in the IDE and upload the program to the Arduino board, the program will tell the Arduino board what to do.[17]

My project uses the Arduino Uno work board, which is the most common entry-level version of Arduino. It has 14 digital input / output pins, 6 analog input pins, a 16 MHz crystal oscillator, and a USB interface, a DC interface, an ICSP interface and a reset button. Just connect it to the USB port of the computer to power it and drive it.

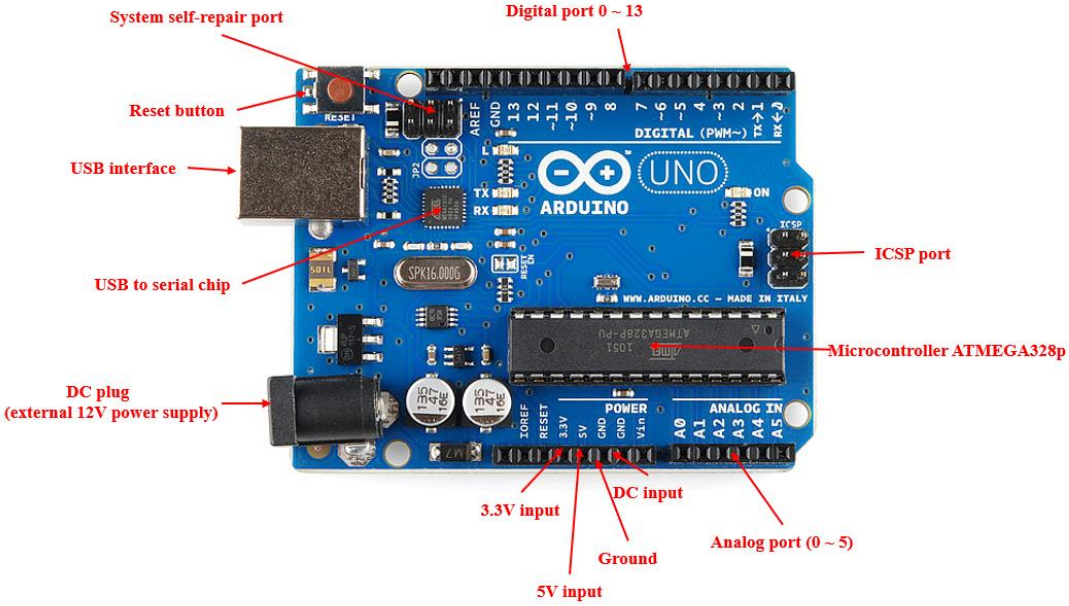

Figure 26 Introduction of Arduino Uno

I can program it through the Arduino IDE on your computer and upload the program to the development board without using an additional editor. Moreover, it can be powered by an external power source such as a battery, and no additional power source is needed.

7.2 LED Display Modules

Display module I used the 4 bits 7 segment display module that comes with the Arduino. Its characteristic is that it can be directly connected to Uno's IO port without any other driver and program buffer. And it needs a 3.3V-5V power supply, and there are two power interfaces on the Arduino Uno, 3.3V and 5V.

7.3 Connection and Programming of Arduino

As seen in the above two figures, connect the 2-9 digital interfaces of the MCU to A-H of the LED display module, and the 10-13 interfaces to the D1 to D4 of the LED. The Vcc of LED is connected to Uno's 3.3V or 5V interface. At this point, the connection between the Arduino Uno and the LED display module is complete.

For a program edited on a computer, a database needs to be established first to correspond to 7 segments on each bit. The following figure shows that 7 segments on a bit correspond to A-H respectively. When displaying special numbers, you only need to call the corresponding segment. For example, if you want it to display “5”, I need to call "A, C, D, F, and G", and the called function can be controlled with "LOW", and what I want to turn off is "HIGH" control.

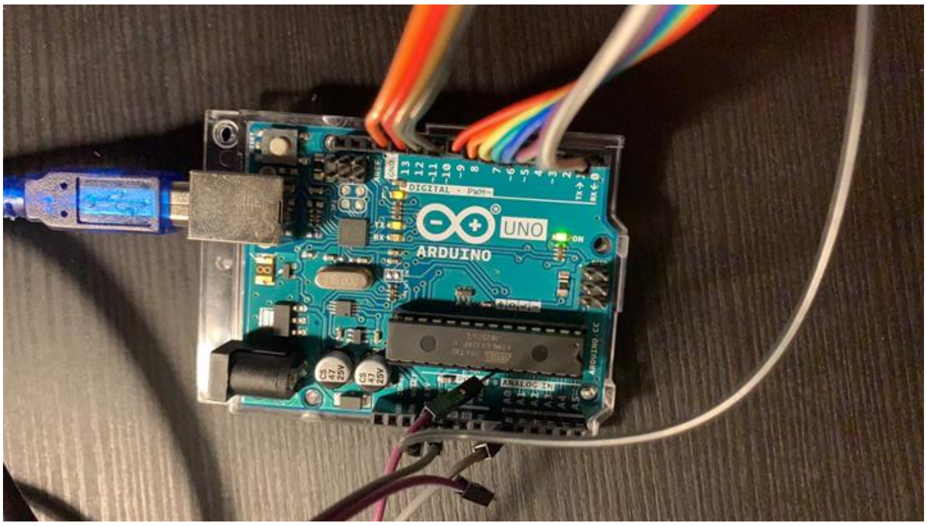

Figure 27 Arduino Uno

Chapter 8 Results and Discussions

This chapter contains the results and analysis of all stages in my research process. The methods of demonstrate all results are displayed as shown in the Flow Chart below.

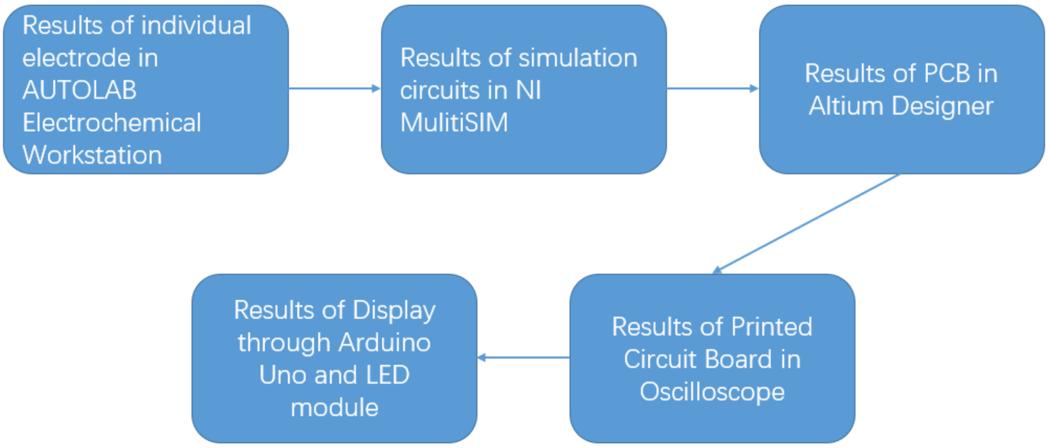

8.1 Results and Discussions of Electrodes Part

8.1.1 Results and Discussions of Saturated Calomel Electrode

As explained in Chapter 3, when testing a saturated calomel electrode, a three-electrode system is connected to the AUTOLAB electrochemical workstation, and the relationship between voltage and time is obtained using the "open potential" function. Then control the reaction concentration and observe the change in the value of the open circuit potential on the electrode at different concentrations.

For this part of the experiment, I used 6 groups of aqueous solutions of sodium chloride with different concentrations. They all passed through the process of filtering out impurities, and their concentrations were 10mmol / L, 20mmol / L, 40mmol / L, 60mmol/L, 80mmol / L and 160mmol / L. As the normal range of sodium ion concentration in human sweat is 30-65 mmol/L, and I thought my samples must contain this range and wider than it for higher accuracy. In addition to the different concentration of the solution, other conditions (including reaction temperature, reaction time (30 seconds), electrode and workstation connection method, etc.) remain unchanged, in this experimental environment, there is only a variable of concentration.

Using the function of 'open circuit potential' in the AUTOLAB electrochemical workstation, the following results were obtained.

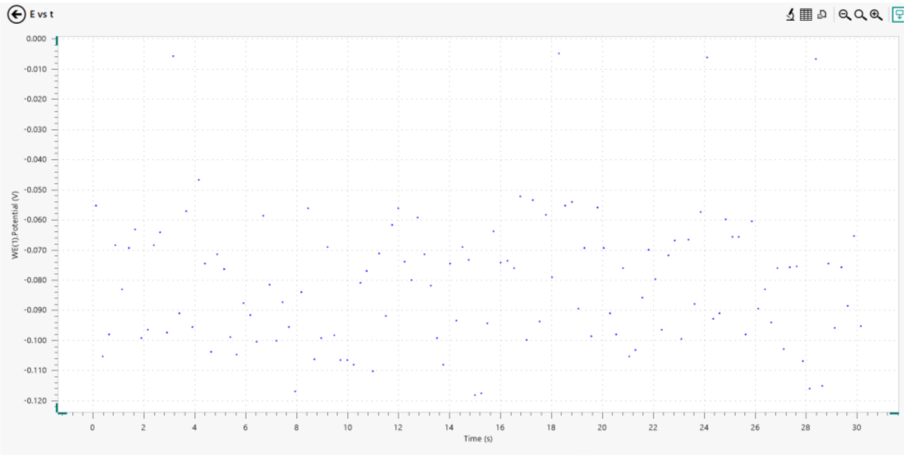

Figure 28 10mmol/L

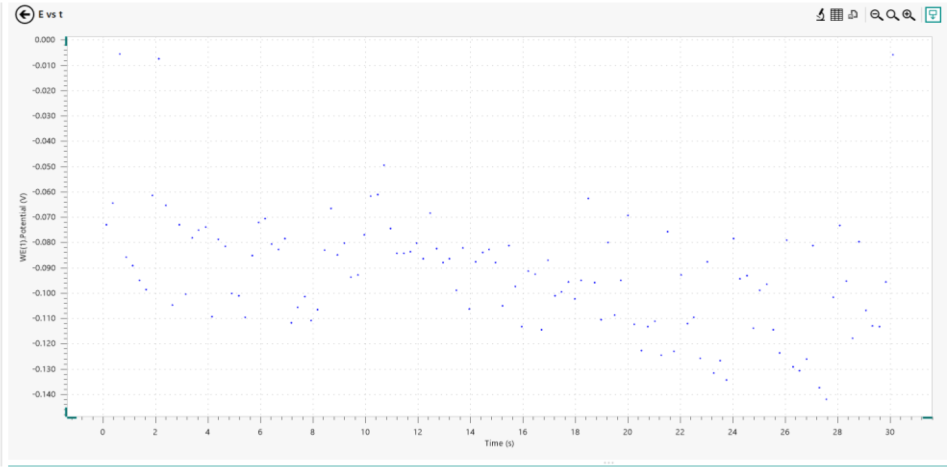

Figure 29 20mmol/L

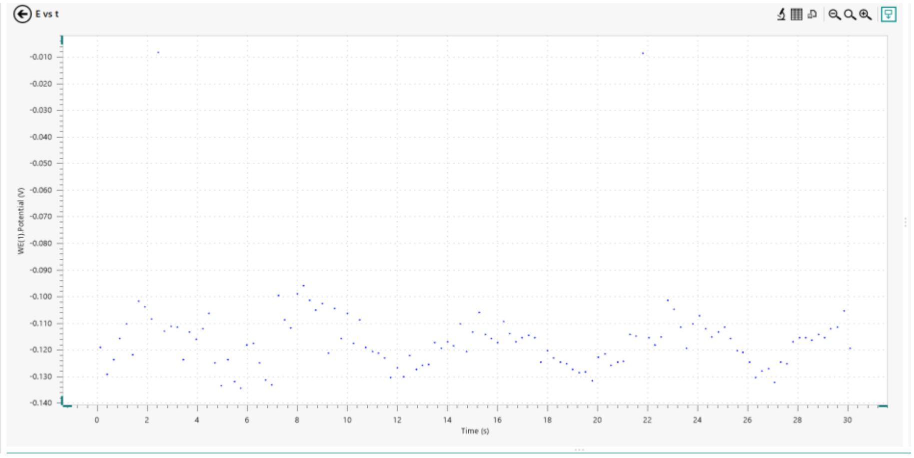

Figure 30 40mmol/L

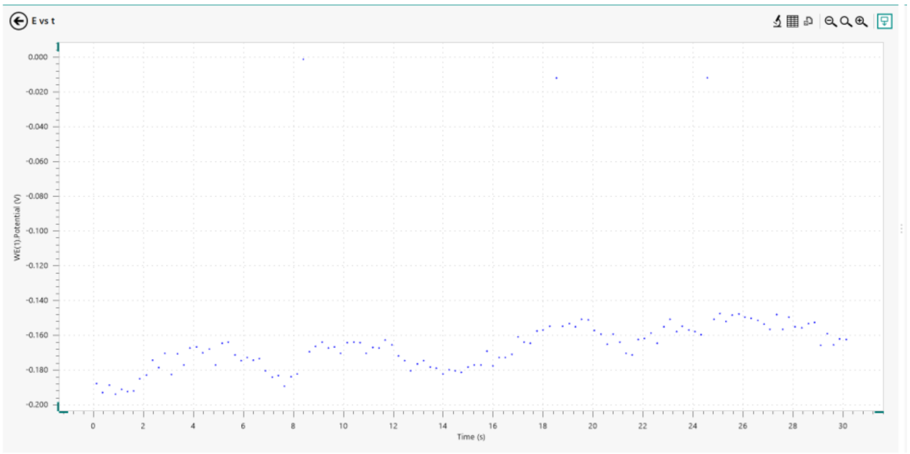

Figure 31 60 mmol/L

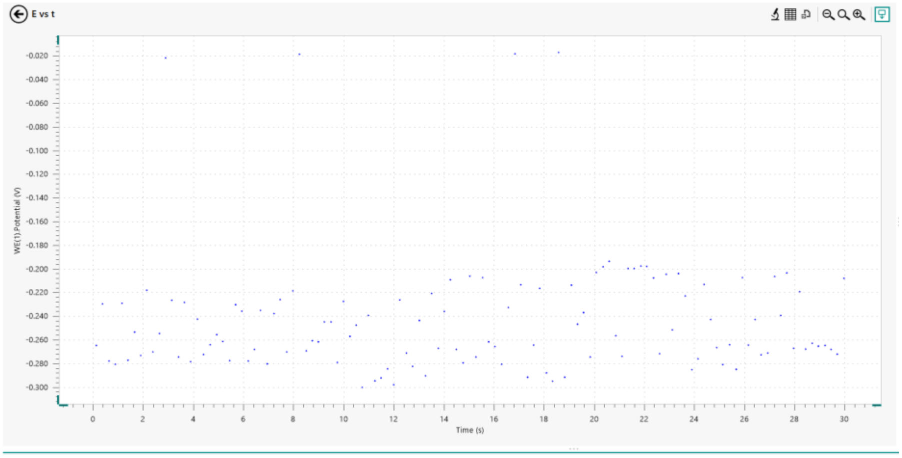

Figure 32 80 mmol/L

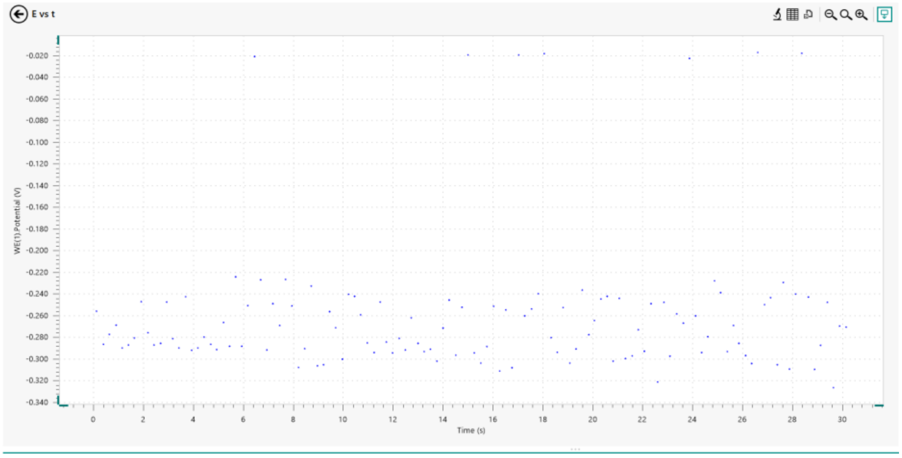

Figure 33 160 mmol/L

s I didn't keep the source files of these data, but I recorded them in logbook every time after experiments. And the numbers of open circuit potential were mean values of 120 times sampling. The following data was obtained from the above results.

Table 4 Results of Saturated Calomel Electrode

Concentration(mol/L)	**0.01**	**0.02**	**0.04**	**0.06**	**0.08**	**0.16**
$\ln[C_{Na^+}]$	-4.60517	-3.91202	-3.2188	-2.8134	-2.52573	-1.83258
Open Circuit Potential (V)	-0.085	-0.105	-0.124	-0.18	-0.265	-0.289

The relationship between the natural logarithm of the concentration of sodium ions in the sodium chloride solution and the open circuit potential can be drawn from the table above.

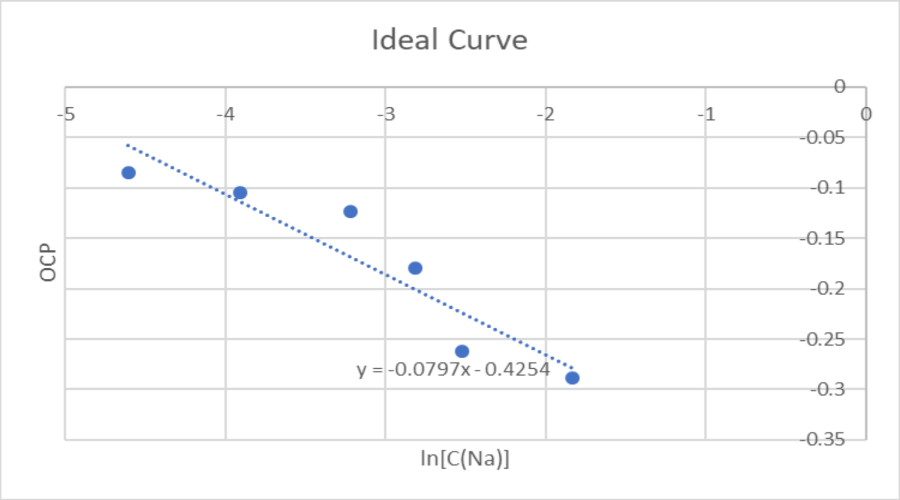

Figure 34 Responding Curve of Saturated Calomel Electrode

It can be seen from this figure that the open circuit potential of the electrode has a linear relationship with the natural logarithm of the sodium ion content in the solution. As the concentration changes, the amplitude of the open circuit potential also changes. It is worth mentioning that the open circuit potentials are all negative and numerically smaller and smaller. The reason for this phenomenon is that in each different electrode system, the potential on the reference electrode is fixed, and this potential value will be different for various electrodes but will not change because of different concentrations. Therefore, when the potential of the working electrode changes, this open circuit potential is the difference between the potential of the working electrode and the potential of the reference electrode. If the potential of the reference electrode is always higher than the potential of the working electrode, this result will be caused. In other words, the sign of the open circuit potential does not represent the direction, but it does represent the magnitude of the amplitude.

It can be seen from the above figure that the Nernst equation of this saturated calomel electrode is:

$$E_{OCP} = -0.4254 - 0.0797 ln\ (C_{Na^+})$$

It can be seen from the above formula that the three-electrode system of the saturated calomel electrode can be described as a linear system. For a solution with unknown sodium ion concentration, the open circuit potential derived from the electrode is substituted into this Nernst equation, the sodium ion concentration of the solution can be calculated.

8.1.2 Results and Discussion of Modified Reference Electrode of Screen-printed Electrode

As described in Chapter 3, before using the screen-printed electrode for the experiment, I modified its reference electrode. It is placed in a sodium chloride solution and then energized to cause an oxidation reaction to oxidize to silver chloride, thereby forming a silver / silver chloride two electrode system. After modifying the reference electrode, I use it as a working electrode to connect to the AUTOLAB electrochemical workstation, and the reference electrode does not connect anything to form a zero-potential point. In this case, the value of the open circuit potential of the workstation is only the valve of the potential of silver chloride on the whole two-electrode system.

I conducted 4 sets of measurements of sodium chloride solution with different concentrations on this electrode.

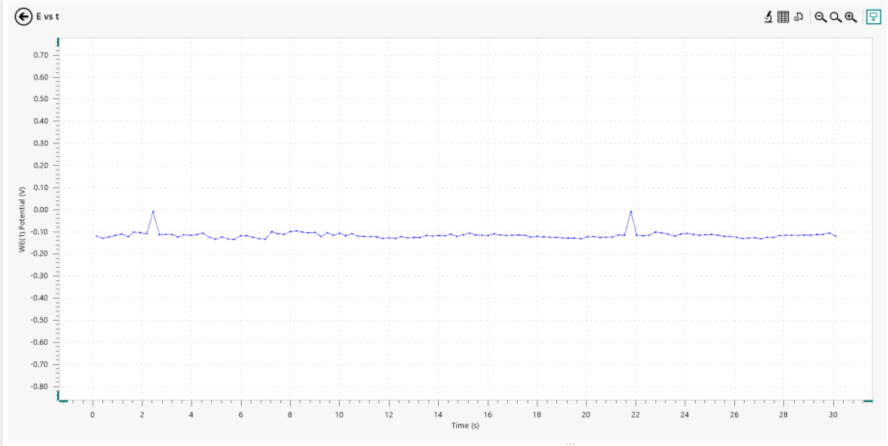

Figure 35 10 mmol/L Sodium Chloride

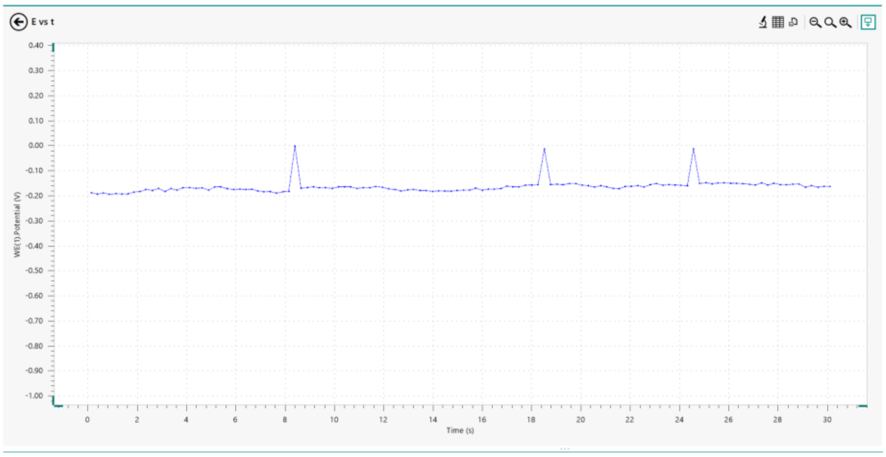

Figure 36 20 mmol/L Sodium Chloride

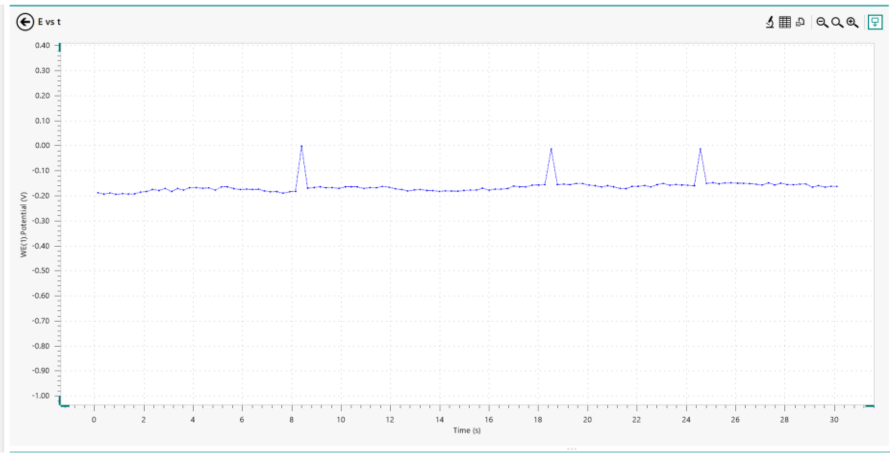

Figure 37 40 mmol/L Sodium Chloride

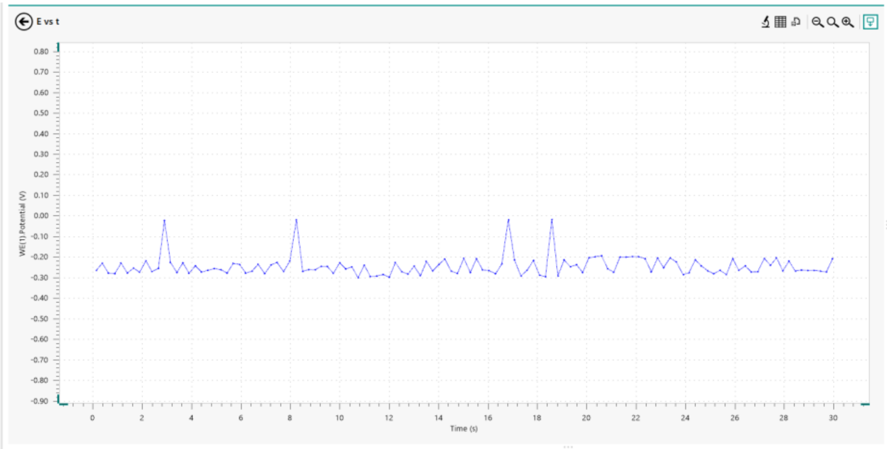

Figure 38 80 mmol/L Sodium Chloride

As can be seen from the four pictures above, no matter how the concentration of the sodium chloride solution changes, the potential on the silver chloride electrode starts to remain around -200mV and does not change with time, keeping it relatively stable. This also proves that the potential of the reference electrode is a fixed value and does not change with the concentration of the measured solution.

8.1.3 Results and Discussions of Screen-printed Electrode

For screen-printed electrodes, I use a two-electrode system connected to the AUTOLAB electrochemical workstation. The same method as the saturated calomel electrode is used to measure the open circuit potential of the solution.

In this group of chemical experiments, all the conditions are the same as the saturated calomel electrode, and the solution is also prepared and stored in an aqueous solution of sodium chloride. In this part, only the electrodes are replaced with screen-printed electrodes.

The following results were obtained by AUTOLAB electrochemical workstation.

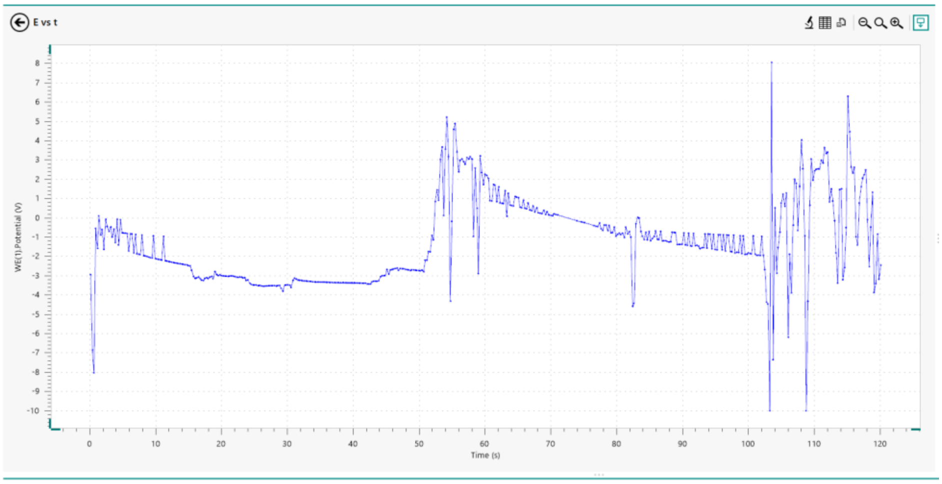

Figure 39 10mmol/L Sodium Chloride

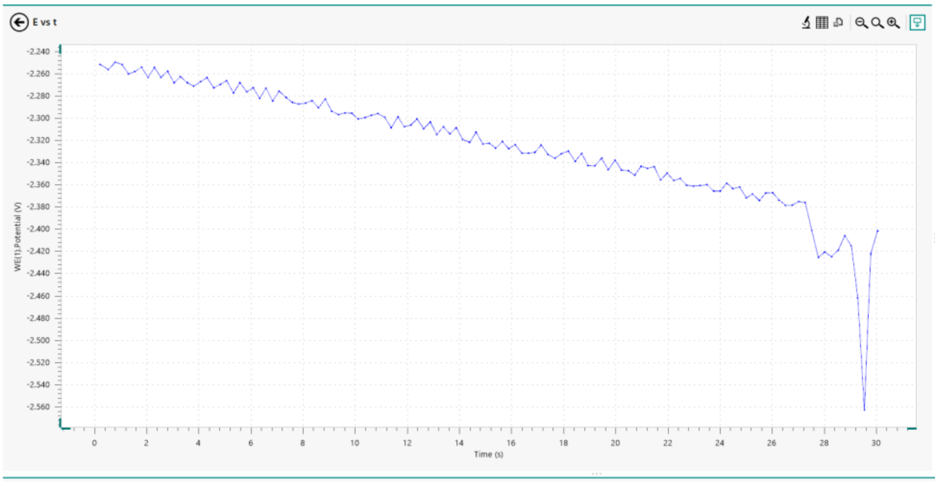

Figure 40 20 mmol/L Sodium Chloride

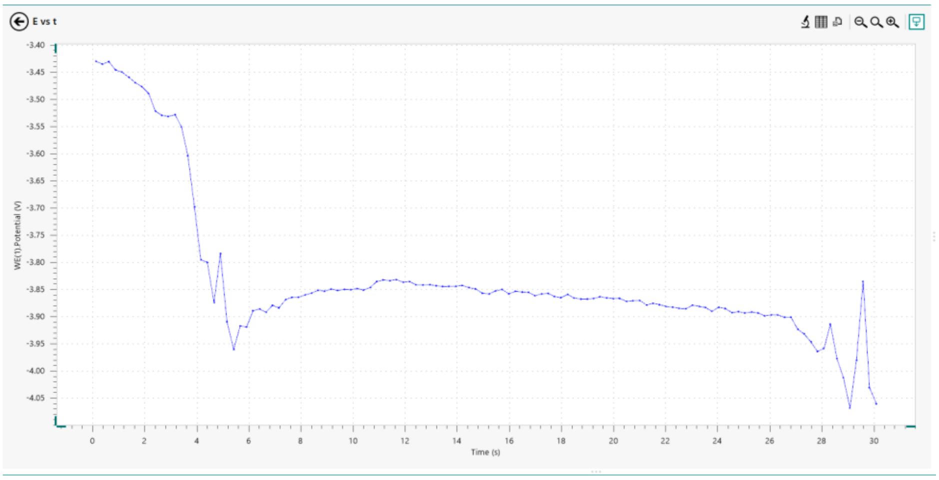

Figure 41 40 mmol/L Sodium Chloride

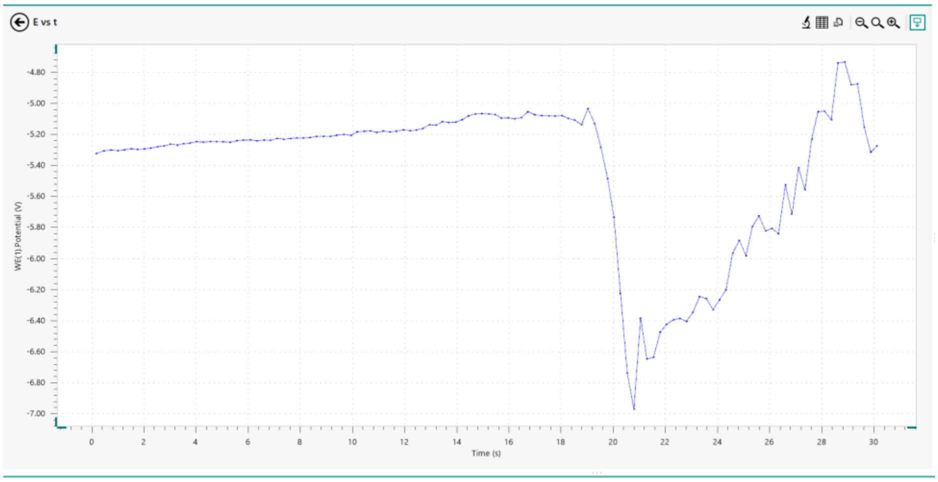

Figure 42 80 mmol/L Sodium Chloride

It can be seen from the results shown in the above figure that no matter how the sodium chloride solution changes, the obtained open circuit potential does not have a reasonable and reliable result. Not only is there no linear relationship with the concentration of sodium ions in the solution, in each experiment conducted at a single concentration, the open circuit potential formed is not expected to not change with time, forming a stable result, but also the changes are non-stop. Such a result is incorrect.

After analysis, the reason for this result is not the solution, but the screen-printed electrode. Since the screen-printed electrode was not modified, I just placed the reference electrode in a sodium chloride solution by conducting electricity to carry out the oxidation reaction and modify it into a silver chloride electrode. Its working electrode does not have an ion selective membrane that allows sodium ions to selectively pass through. In this case, not only does the reaction of sodium ions to obtain electrons reduced to sodium crystals occur on the working electrode, but the following reaction also occurs.

$$H^+ + e^- \to H_2$$

Hydrogen ions in the free state in the water will also get electrons, a reduction reaction will occur, and this process will also release electrical potential. Moreover, this potential is disorderly and irregular, because the content of hydrogen ions in water is not fixed, but changes continuously following the progress of the reaction. It can be seen from this that if the working electrode of the screen-printed electrode is unmodified, it cannot be specifically identified with the sodium ions in the solution, and only the value of the potential of the sodium ion reduction reaction is collected. This result is definitely meaningless.

8.1.4 Results and Discussions of Modified Screen-printed Electrode

As introduced in Chapter 3, this part of my research uses a commercially modified screen-printed electrode connected to the AUTOLAB electrochemical workstation for reaction.

Unlike the previously reacted sodium chloride solution, the solution used in this section was reformulated and the sample solution was sent to Flinders Analytical for quantitative analysis. Hence, the concentration of sodium chloride solution used in this experiment is very accurate. I used 5 sets of samples, their concentrations were 13.75 mmol / L, 29 mmol / L, 62.32 mmol / L, 88 mmol / L and 154.1 mmol / L. Except for different concentrations, the remaining conditions remain the same as in previous experiments.

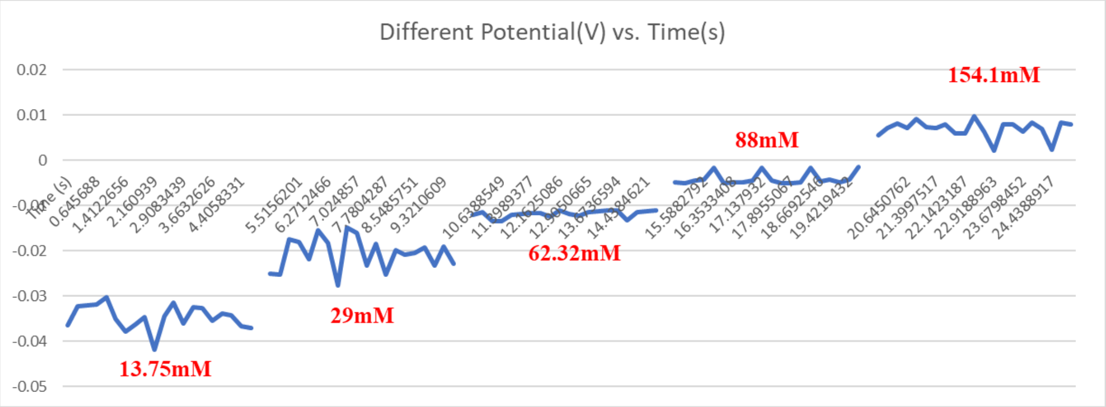

Figure 43 Results of Modified SPE

As can be seen from the above figure, the electrode has an open circuit potential output that is separated from each other in different concentrations of sodium chloride solution and changes as the concentration changes. I did not keep the original image, but took the same data within 5 seconds for each set of data, and placed the 5 sets of sample data on a graph, so that a "separation" trend can be seen more intuitively. These data are the weighted averages I obtained after repeating 6 experiments. The results of this weighted average are listed in the table below.

Table 5 Results of Modified Screen-printed Electrode

Concentration(mol/L)	**0.01375**	**0.029**	**0.06232**	**0.088**	**0.1541**
$ln[C_{Na^+}]$	-0.428672	-3.54046	-2.77547	-2.43042	-1.87015
Open Circuit Potential (V)	-0.03563	-0.02071	-0.00953	-0.00413	0.007162

The open circuit potential output from the workstation has a linear relationship with the natural logarithm of the sodium ion concentration. And this linear relationship can be returned to an equation, which is the special Nernst equation of this electrode.

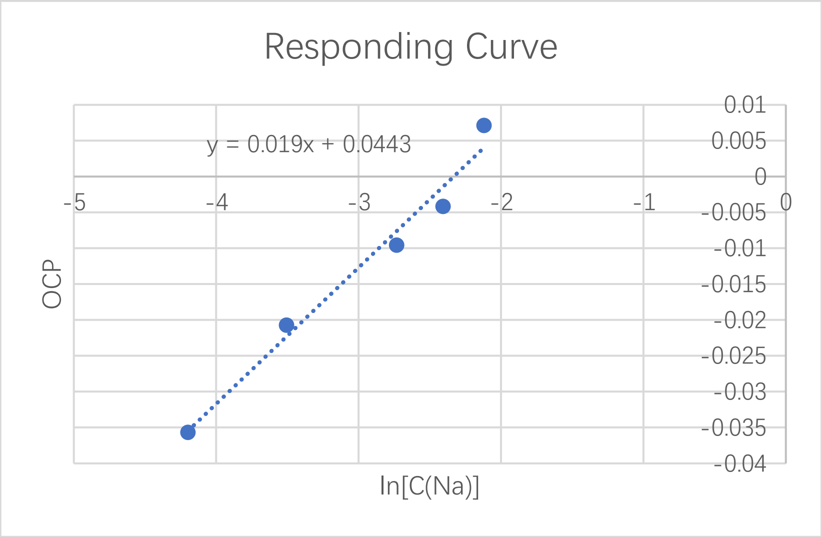

Figure 44 Responding Curve of Modified SPE

As can be seen from the above figure, as the concentration of sodium ions in the solution increases, the open circuit potential of its output shows a rising trend and crosses the positive and negative quadrants. It can be seen that not only the trend of the Responding Curve of the saturated calomel electrode is different, but the quadrant where the results are located is also different. The possible reason for this result is the constant potential of the reference electrode in the two-electrode system. The magnitude of the electric potential determines the value of the final open circuit electric potential. Because the open circuit potential is the potential of the working electrode minus the potential of the reference electrode, the final result can have a positive value.

The specific Nernst Equation is:

$$E_{OCP} = 0.0443 + 0.019ln\,(C_{Na^+})$$

Similar to the saturated calomel electrode, for a solution with unknown sodium ion concentration, the open circuit potential is measured, and then the Nernst equation is used to calculate the concentration of sodium ion in the solution.

8.1.5 Comparison between Three Different Electrode

Table 6 Comparison between Three Different Electrodes

Types of electrodes	**Traditional saturated calomel electrode**	**Screen-printed electrode**	**Commercial Modified SPE**
Advantages	It can specifically recognize sodium ions in solution.	Its small size and thinness make it very suitable as a wearable device.	Small size and reaction with sodium ion specifically.

Disadvantages	Its volume was too large to be a wearable device.	One-off. Unmodified electrodes cannot react only to sodium ions in solution.	The recognition range seems to be limited, and the accuracy is not enough at high concentrations.

The goal of the first part of my research is to test and find the most suitable electrode for my project through a large number of electrochemical experiments. By comparing the above three electrodes, the modified screen-printed electrode is most suitable for my sensor device because its volume is suitable for a wearable device and can be used multiple times. And the silver chloride electrode is very stable and is less affected by the external environment. The most important thing is that it can specifically react with sodium ions in the solution without interference from other redox reactions in the solution. Therefore, in my next experiment, I used this modified screen-printed electrode.

8.2 Results and Discussions of Simulation of Function Circuit

As introduced in Chapter 5, after completing the design of the circuit, I use computer software to simulate its function and observe whether the circuit can perform the corresponding function.

8.2.1 Results of Oscilloscope

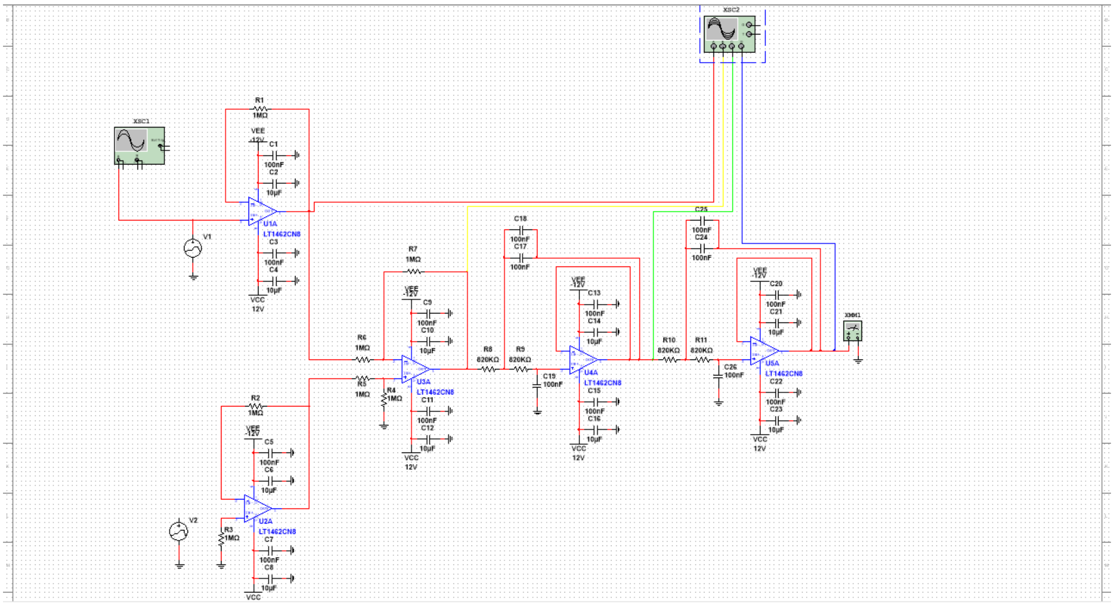

Figure 45 Connection of Oscilloscope

First, connect the oscilloscope, and then run the circuit. I connected the source signal and the output of each section of the circuit to the oscilloscope, so that you can intuitively observe the results of the source signal waveform after passing through different circuits.

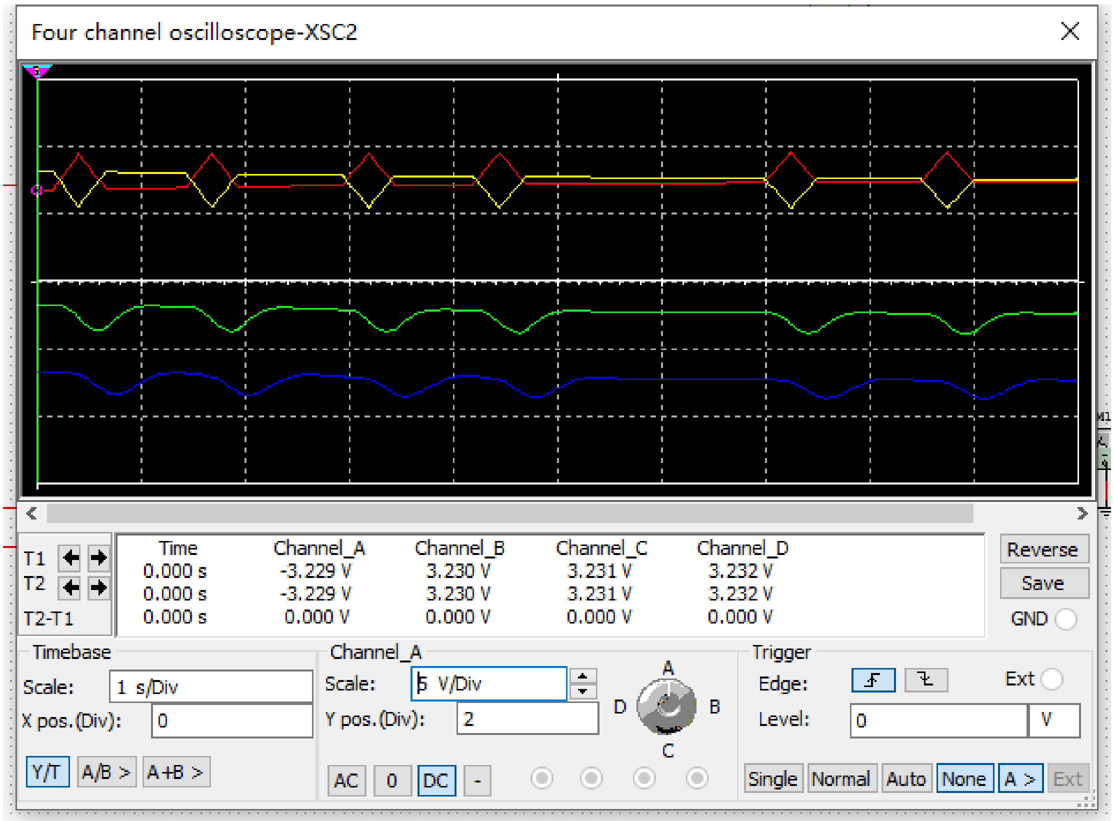
Four channel oscilloscope-XSC2

	Time	Channel_A	Channel_B	Channel_C	Channel_D
T1	0.000 s	-3.229 V	3.230 V	3.231 V	3.232 V
T2	0.000 s	-3.229 V	3.230 V	3.231 V	3.232 V
T2-T1	0.000 s	0.000 V	0.000 V	0.000 V	0.000 V

Timebase
Scale: 1 s/Div
X pos.(Div): 0

Channel_A
Scale: 5 V/Div
Y pos.(Div): 2

Trigger
Edge:
Level: 0 V

Figure 46 Results of Oscilloscope

The figure above shows the result of the oscilloscope. The red line in the figure is the source signal. It can be seen that the source signal has very obvious sharp peaks. These peaks are the inevitable high-frequency noise in the experiment, which interferes with the signal. The yellow line in the figure is the waveform after the voltage buffer. It can be observed that except for the direction of the wave becoming opposite, the amplitude has not changed. The value of changes from the second quadrant to the first quadrant, which is convenient for later input to the display module for display. The green line in the picture is the image after the subtractor. It can be seen that the amplitude is very different from the previous yellow line, and when I designed the circuit before, each LT1462 power interface was connected in parallel with two capacitors with different capacitances which are used for preliminary filtering. It can be seen from the difference between the green line and the yellow line that the effect of the initial filtering is still obvious, and the peak of the wave is obviously not as sharp as before. The blue line in the figure is the final output signal. It can be seen that the final output signal is very flat and the interference is very small. It can be concluded that such a result is acceptable in later work, which can be judged that the functional circuit can realize the expected function at design time.

It is worth mentioning that the amplitude of the voltage after the subtractor has not changed significantly. This is also mentioned in the design chapter. I did not design the circuit gain very large. The excessive output voltage caused by the gain will have a negative influence on the LT1462 in the circuit. After all, the LT1462 is an op amp that works under microampere. Hence, for the weak open circuit potential directly collected by the electrode, how to display this value is also a tricky task, which will be explained in Chapter 7.

8.2.2 Results of Bode Plotter

After observing the result with an oscilloscope, I connected a Bode plotter to observe the frequency characteristics between the input signal and the output signal.

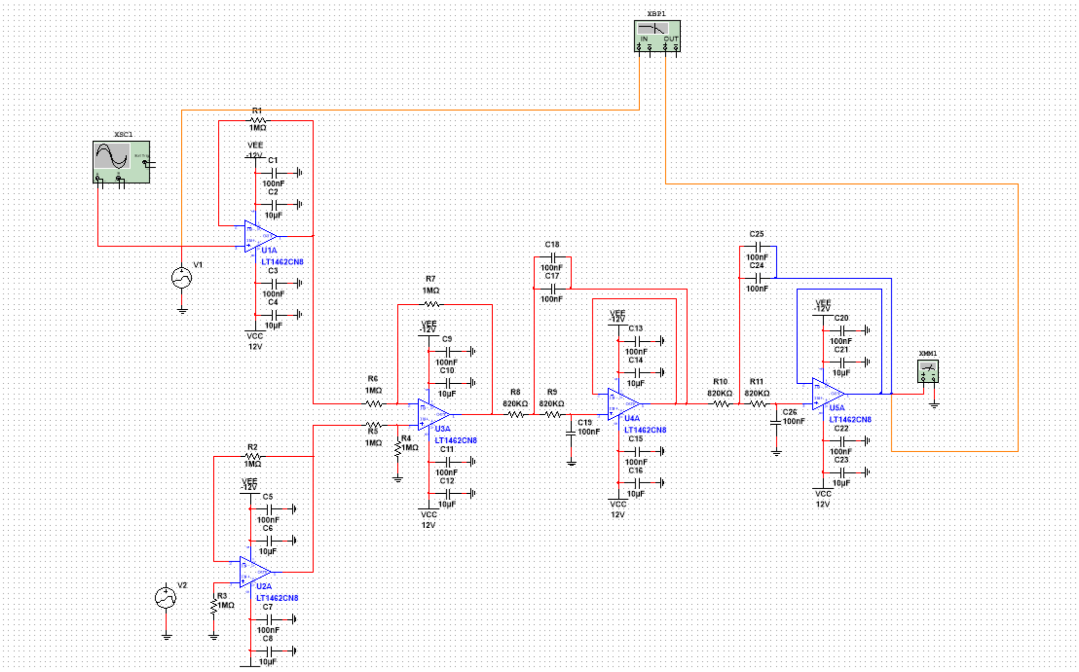

Figure 47 Connection of Bode Plotter

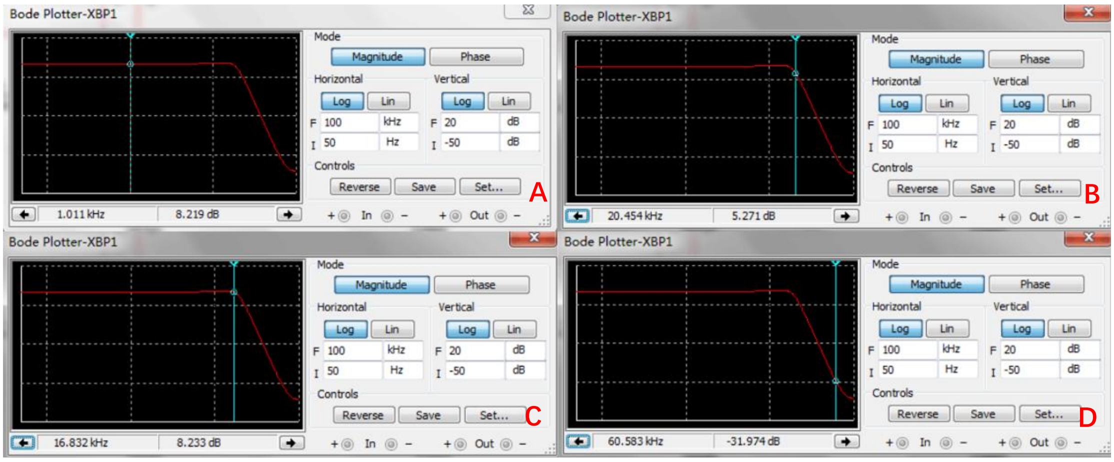

A: Horizontal F 100 kHz, I 50 Hz; Vertical F 20 dB, I -50 dB; 1.011 kHz 8.219 dB

B: Horizontal F 100 kHz, I 50 Hz; Vertical F 20 dB, I -50 dB; 20.454 kHz 5.271 dB

C: Horizontal F 100 kHz, I 50 Hz; Vertical F 20 dB, I -50 dB; 16.832 kHz 8.233 dB

D: Horizontal F 100 kHz, I 50 Hz; Vertical F 20 dB, I -50 dB; 60.583 kHz -31.974 dB

Figure 48 Results of Bode Plotter

The picture above is the result of a Bode plotter. As can be seen from the first result, the corresponding logarithmic coordinate is 8.219dB, and the minus 3dB is the corresponding cut off frequency. Therefore, the corresponding cut-off frequency on the Bode plotter should be the frequency of 5.219dB on the ordinate, which can be seen from the second picture about 20.454kHz, which is the same as the theoretically expected value. And when the frequency begins to decay, as shown in the third picture, the frequency that begins to decay is 16.832kHz. When the frequency is adjusted to 60.583kHz, the corresponding ordinate is -31.974dB, which shows that the filter can effectively attenuate high-frequency signals and has good filtering characteristics.

At this point, the simulation of the circuit has been completed. The next step of my research is to make it into a printed circuit board (PCB), and connect the manufactured board with the electrodes to test at the hardware level.

8.3 Results and Discussions of the Assembled Device

After the production of the PCB and the welding of the components are completed, the completed circuit board is connected to the modified screen-printed electrode selected in the first part, and is powered by a 10V voltage regulator. The difference with the first part is that I used the final result on the oscilloscope in the laboratory instead of the AUTOLAB electrochemical workstation. Because AUTOLAB has its own functional circuits, and these circuits process the signals collected by the electrodes and then display them as the final open circuit potential on NOVA. However, it is no longer possible to connect the AUTOLAB workstation to allow the system composed of electrodes and circuits to work independently.

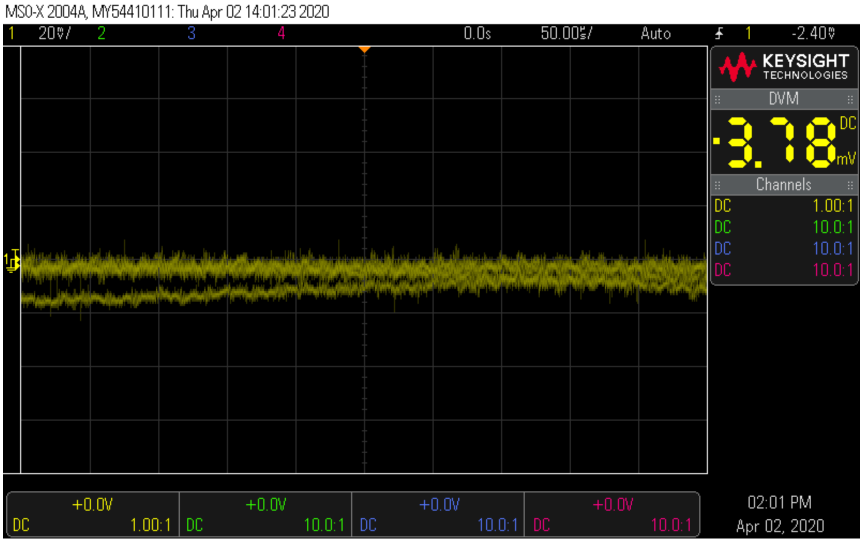

Figure 49 Only Electrode in Oscilloscope

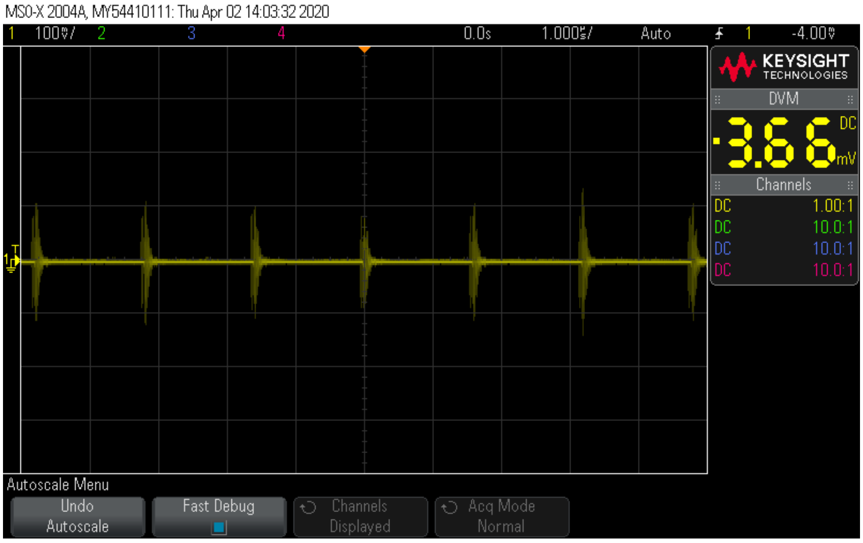

Figure 50 Electrode and Circuit Board in Oscilloscope

The two figures above are the results displayed by the oscilloscope.

The first picture is a result diagram with only electrodes connected. It can be seen that the resulting signal is very noisy and unstable, and the resulting waveform is constantly oscillating. The scan frequency is 50uV/s and the -3.78mV is the output open circuit potential. Obviously, such a result cannot be used. Although the average value of the voltage given by the oscilloscope is reliable, the expected signal result graph should be relatively stable at a certain value.

The second picture is the result of connecting the electrodes to the circuit board. It can be seen that the signal after the functional circuit becomes very stable and the waveform does not have any oscillation. Such a result can be received, and just as the gain was not set too large when designing the circuit, the final open-circuit potential result is similar in amplitude to the electrode-only result.

When looking for the specific Responding Curve and Nernst equation of this assembled device, I also used an aqueous solution of sodium chloride crystal directly as the sample to be tested. The samples I used were also used in the third electrode experiment, and their concentration was measured and determined by Flinders Analytical.

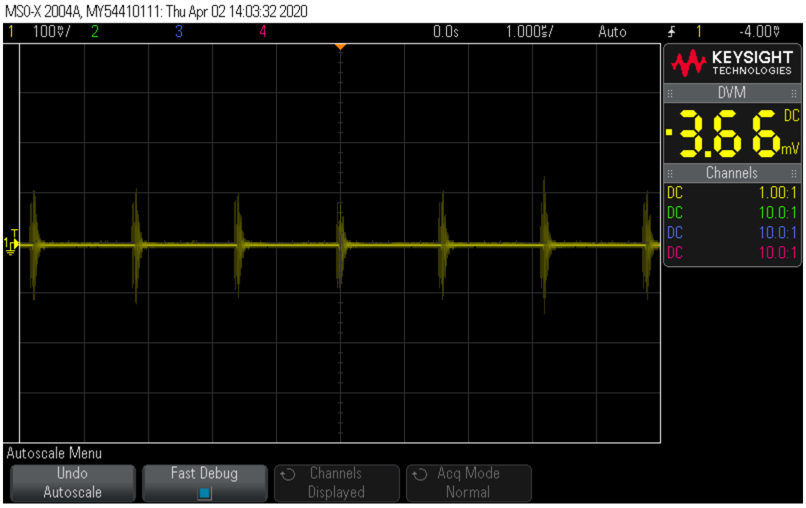

Figure 51 13.75mmol/L Result in Oscilloscope

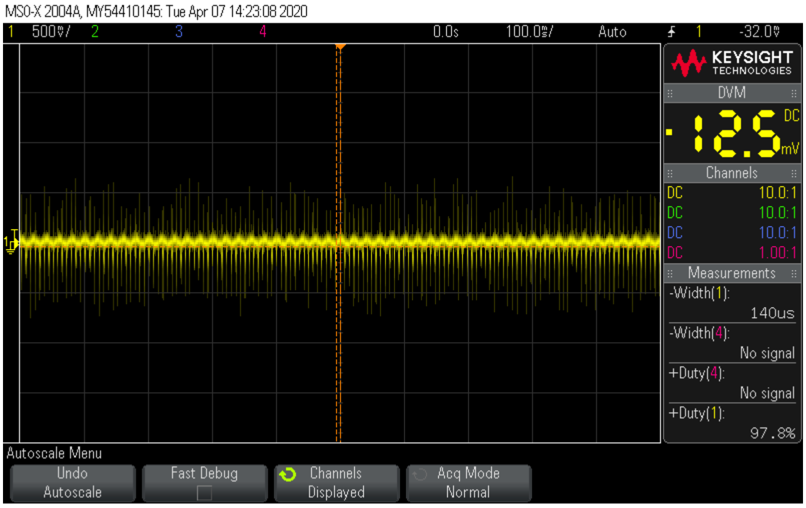

Figure 52 29mmol/L Result in Oscilloscope

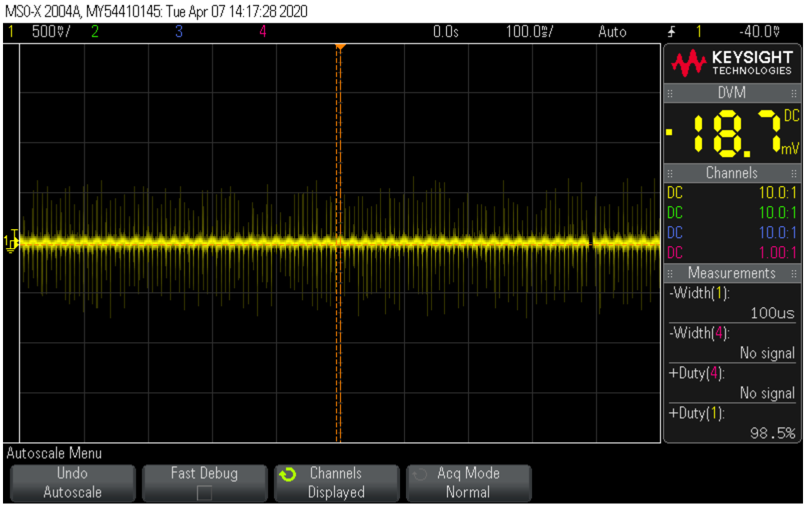

Figure 53 62.32mmol/L Result in Oscilloscope

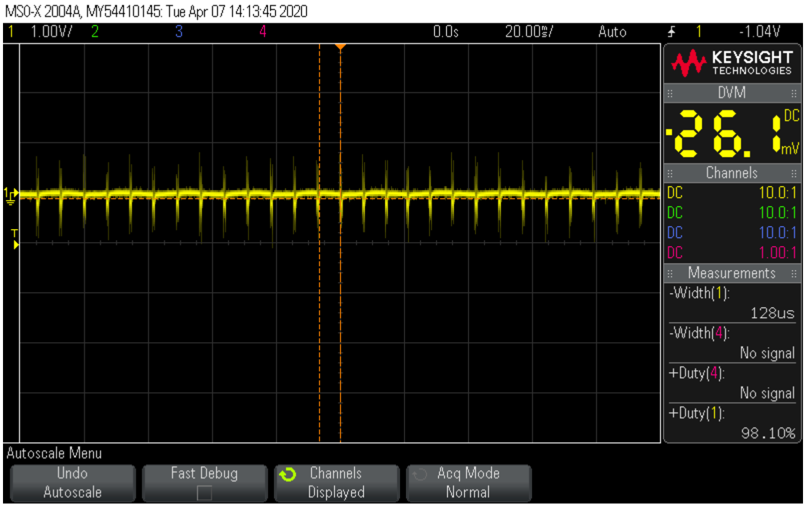

Figure 54 88mmol/L Result in Oscilloscope

The following data was obtained from the above results.

Table 7 Results of Assembled Device

Concentration (mol/L)	**0.01375**	**0.029**	**0.06232**	**0.088**
$ln[C_{Na^+}]$	-4.28672	-3.54046	-2.77547	-2.43042
Open Circuit Potential (V)	-0.00363	-0.0125	-0.0187	-0.0261

The Responding Curve drawn from the table above:

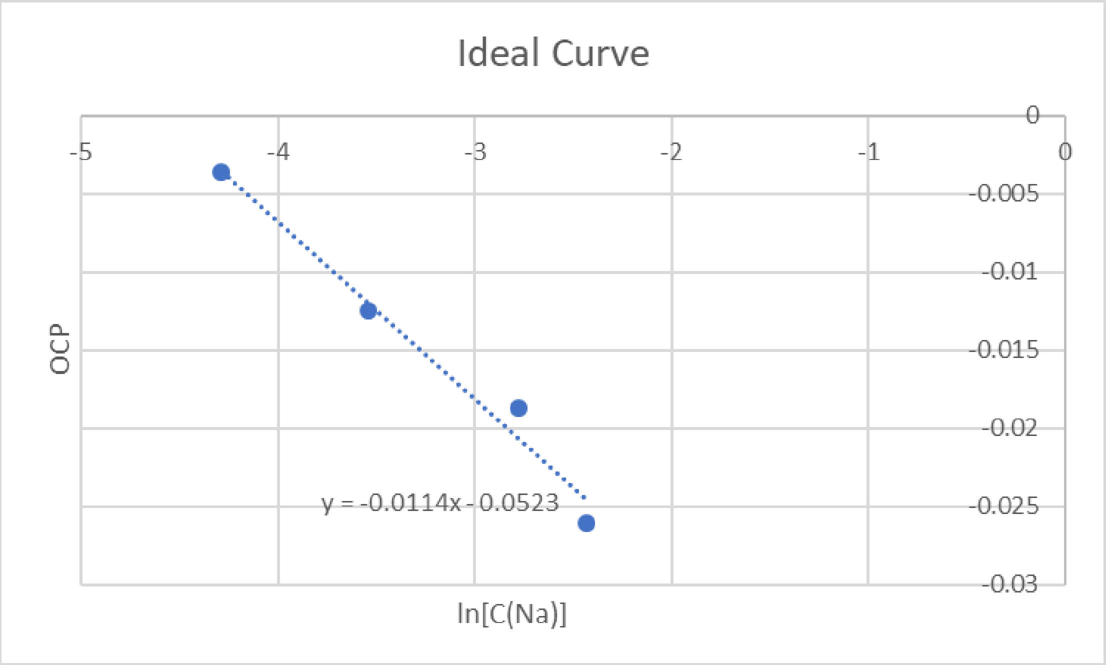

Figure 55 Responding Curve of Assembled Device

And the specific Nernst Equation:

$$E_{OCP} = -0.0523 - 0.0114 ln\,(C_{Na^+})$$

The above-mentioned Nernst equation can be regarded as the specific Nernst equation of this assembled device, and this equation can be used to calculate the sodium ion concentration by measuring the open circuit potential of a solution of unknown sodium ion concentration.

8.4 Results Calibration and Possible Problems

However, it can be seen that the above Responding Curve does not have the sample of 154.1 mmol / L previously placed in the Responding Curve. In fact, I also did repeated experiments in the completion of the above results. Observe that the samples that disturb the label are randomly selected to test the open circuit potential and use the open circuit potential to calculate the sodium ion concentration. Low concentration solutions can complete the result calibration, but after increasing the concentration, the results show that they become very unstable.

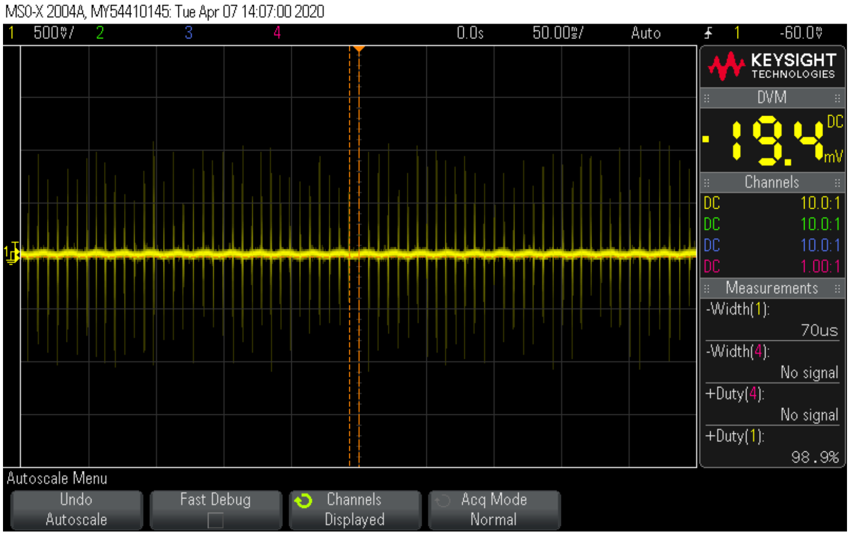

MSO-X 2004A, MY54410145: Tue Apr 07 14:07:00 2020

Figure 56 154.1mmol/L Result 1

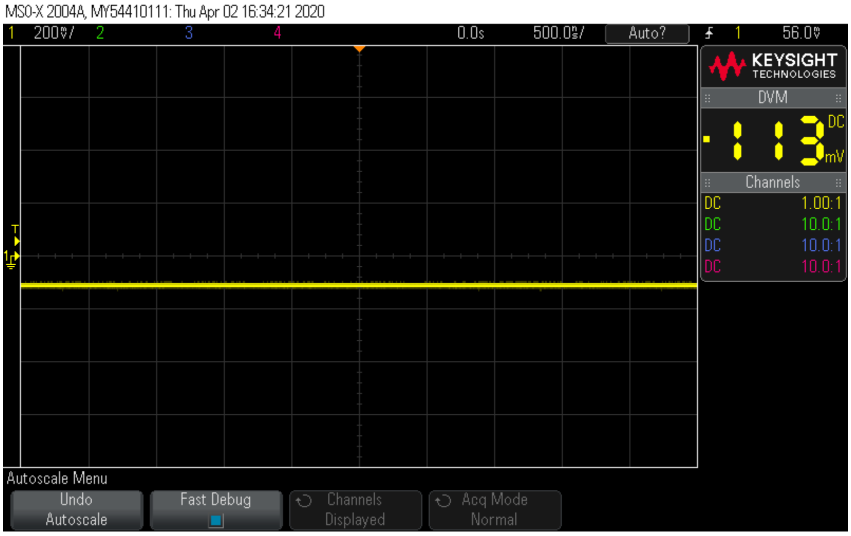

MSO-X 2004A, MY54410111: Thu Apr 02 16:34:21 2020

Figure 57 154.1mmol/L Result 2

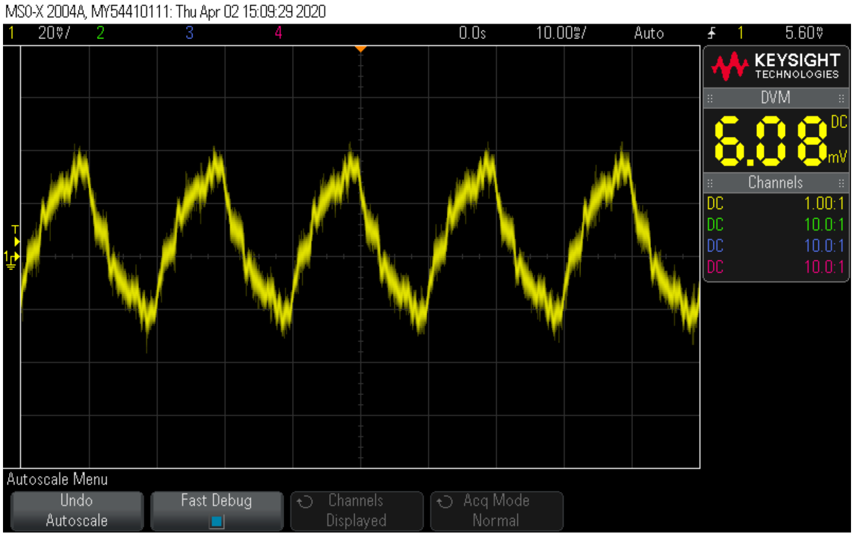

MSO-X 2004A, MY54410111: Thu Apr 02 15:09:29 2020

Figure 58 154.1mmol/L Result 3

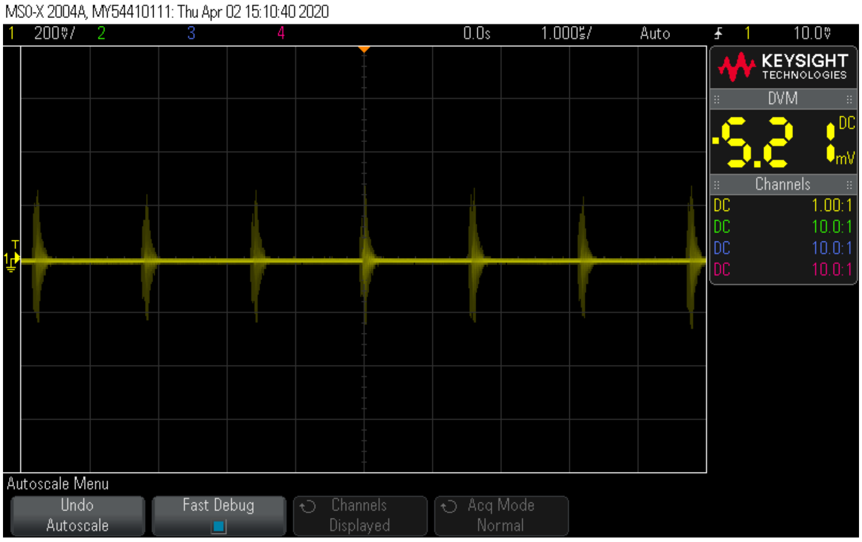

Figure 59 154.1mmol/L Result 4

The four pictures above are the open circuit potentials of a sodium chloride solution with a concentration of 154.1 mmol / L measured at different times. It can be deduced from the above Nernst equation that if the concentration is 154.1 mmol / L, the expected open circuit potential result should be:

$$E_{OCP} = -0.0523 - 0.0114ln(0.1541) = -0.03098V = -30.98mV$$

The above results did not fall within the expected range, and the reasons for this result, according to my analysis, there are the following points.

(1) The excessively high concentration of the solution exceeds the threshold of the detection range of the electrode.

The normal range of sodium ions in human sweat is 30-65 mmol / L, and the content of sodium ions in normal human sweat is about 40 mmol / L. Subjects whose sodium ion concentration exceeds 65 mmol / L can be called hypernatremia or have a potential risk of cystic fibrosis. In other words, the sodium ion content in normal human sweat does not reach as much as 154mmol / L. This modified screen-printed electrode is the electrode in the commercial small blood sodium meter I bought. It is also designed to detect the content of sodium ions in human blood. The threshold of electrode design may not have such a high concentration.

(2) The LT1462 op amp in the circuit was destroyed.

As I said before, I did not design the gain of the differential amplifier circuit very large at that time because I was afraid that the output voltage would be too high and might exceed the tolerance range of the LT1462. Through the LT1462 datasheet, the maximum pass current of each amplifier is 45μA. When the concentration of sodium ions in the measured solution is too high, the current flowing into the circuit is too large and the LT1462 op amp is overloaded and loses its function. This is the worst result because such an error cannot be repaired, and a new circuit board needs to be replaced.

(3) High-concentration solutions take longer to reach a stable state.

When designing the electrochemical experiment, I did not design the reaction time as a variable, but set the time to a fixed value. Because most solutions are stable in a similar time. Because of the length of the reaction time, it is the saturated calomel electrode that affects the experimental results, because the potassium chloride crystals in it will crystallize in the solution for a long time, which will affect the experimental results. Under normal circumstances, this does not happen with screen-printed electrodes. In this case, it cannot be ruled out that the solution with too high concentration will cause sodium chloride crystals to be precipitated due to long-term storage, and the collected solution is not actually the solution with the expected concentration.

8.5 Results and Discussions of Arduino MCU and LED Display

The resolution of Arduino Uno is 10 bits, so the integer value is from $0 - 2^{10}$ = 1024. The voltage of 5V is assigned to 1024, so Uno can be displayed as a minimum of 0.005V.

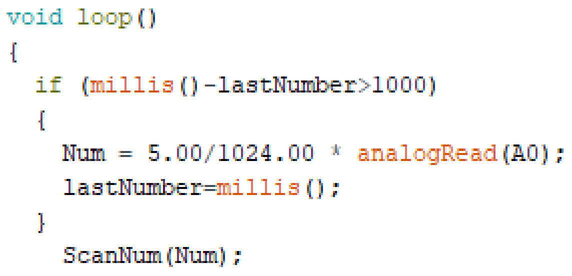

```
void loop()
{
  if (millis()-lastNumber>1000)
  {
    Num = 5.00/1024.00 * analogRead(A0);
    lastNumber=millis();
  }
    ScanNum(Num);
```

Figure 60 Programming of Arduino IDE

When directly connected, the displayed voltage value is the converted hexadecimal value, that is, 5V displays "1024". In order to display it as a normal decimal voltage value, I used the one shown above and multiplied by $\frac{5.00}{1024.00}$. In this case, the output result becomes a decimal voltage value.

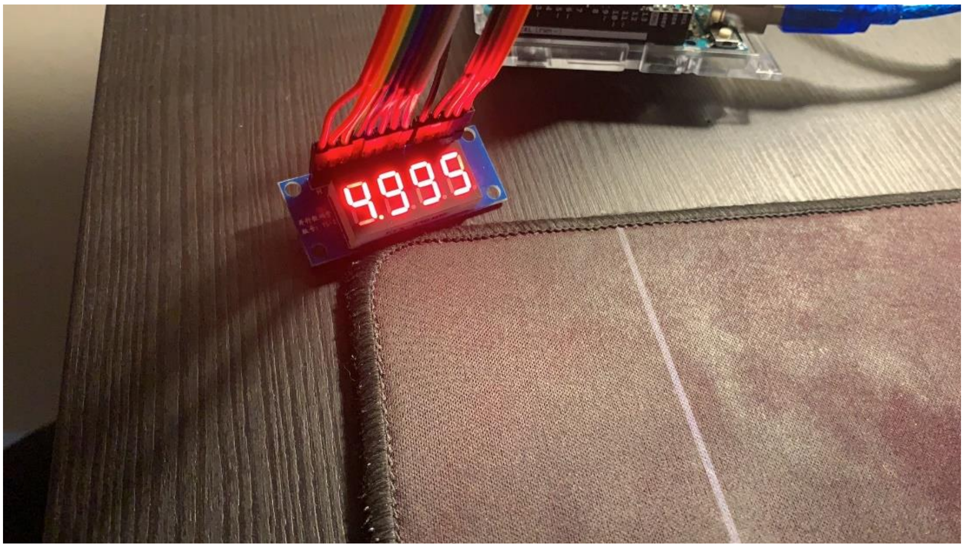

Figure 61 LED Displays 5V

The picture above is the result when the program I designed displays 5V, and the final LED display module displays "4.995". This is the result of its accuracy of 0.005.

However, the amplitude of the output open circuit potential of my research project is in the microvolt level, and the error of five thousandths is too large for this result, which will affect the accuracy of the final result. For my project, the expected results should be accepted at 1 in 10,000. This is because the Arduino Uno only has 14 IO interfaces, and there is no redundant interface for additional precision reduction operations.

However, this part work provides a possibility of using an Arduino microcomputer to control an LED display module to display voltage. In the future work, I can use Arduino Mega with more IO interfaces to display with higher precision.

Chapter 9 Conclusion

This article builds a framework for a new wearable sweat sodium detection device. Existing wearable detection devices are mostly physical feedback sensors based on physical responses such as heart rate or pulse. They cannot analyse the health status of the human body at the molecular level. Instruments with molecular level analysis, such as blood glucose meters, are invasive. This article creates a new detection method, which uses sodium ion selective electrodes to detect the sodium ion content in the solution, and then uses a functional circuit to process it, and analyses the human body condition through the output results. This sensor combines the technology of electrodes in electrochemistry, the technology of signal processing in electronic circuits and the technology of circuit board fabrication, and a microcomputer program is used to control the LED display in the display module.

- In the electrode’s selection and testing

By testing three different types of electrodes on the market and testing their properties, it was found that they all have their own characteristics, advantages and disadvantages.

The saturated calomel electrode can react with the sodium ions in the solution to detect its content, but the saturated calomel electrode cannot be used as part of the wearable device because of its volume and other factors. Although the screen-printed electrode is small in size and light in weight, it cannot specifically bind sodium ions in solution. It is not only the potential released by the reduction reaction of sodium ions at its working electrode. The modified screen-printed electrode finally adopted has a layer of sodium ion selective ionophore on its working electrode surface, which combines with sodium ions and passes through the selective membrane to stay on the working electrode surface. Therefore, the potential on the working electrode is only the potential generated by the reduction reaction of sodium ions.

- In the function circuit establishment

Since the signal collected by the electrode is very weak and unstable, the intervention of the functional circuit is to stabilize the open circuit potential signal obtained by the electrode, and perform a subtraction operation between the signal of the working electrode and the signal of the reference electrode.

The design of the voltage buffer circuit is to buffer the signals collected by the electrodes. The ultra-high output impedance is designed so that the signal is not affected by the second stage circuit. At the same time, two identical buffer circuits can simultaneously collect potential signals on the working electrode and the reference electrode. The subtractor circuit is to subtract the two signals. Because the definition of open circuit potential is the voltage on the working electrode minus the voltage on the reference electrode. The fourth-order low-pass Butterworth filter is designed to filter out the interference of high-frequency signals in the circuit.

After completing the design of the circuit and the simulation of the software, Altium Designer is used to make a printed circuit board and solder the components on the circuit board. Combining the obtained circuit with the electrode to carry out experiments to obtain its specific Responding Curve and Nernst equation.

The advantage of this wearable sensor is real-time detection and is non-invasive. The design of the functional circuit can effectively optimize the collected signal, so that the result becomes stable and small fluctuation. The LED module driven by Arduino can effectively and intuitively display the digital potential results.

Chapter 10 Future Work and Prospect

This chapter introduces the work can be extended, and the work can be completed in future work. In addition, this chapter also introduces the prospects of this project.

10.1 Future Work

As I introduced in the previous chapter, electrodes and circuit board assembled equipment lose accuracy for high-concentration solutions. The next work requires repeating experiments with different circuit boards to find out the cause of this result shift.

In addition, the original design of this research project used flexible materials to print circuit boards, using thermoplastic polyurethane (TPU) as the substrate, and nano-silver materials as ink to print the circuit. However, due to the closure of the laboratory of La Trobe University with Dimatix, this work was not completed.

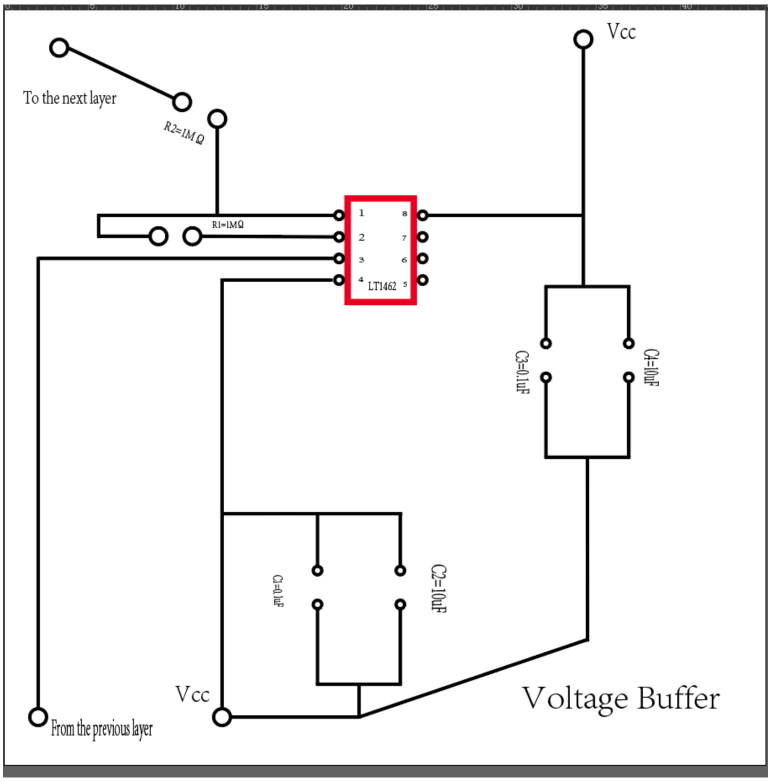

Figure 62 Voltage Buffer in AI

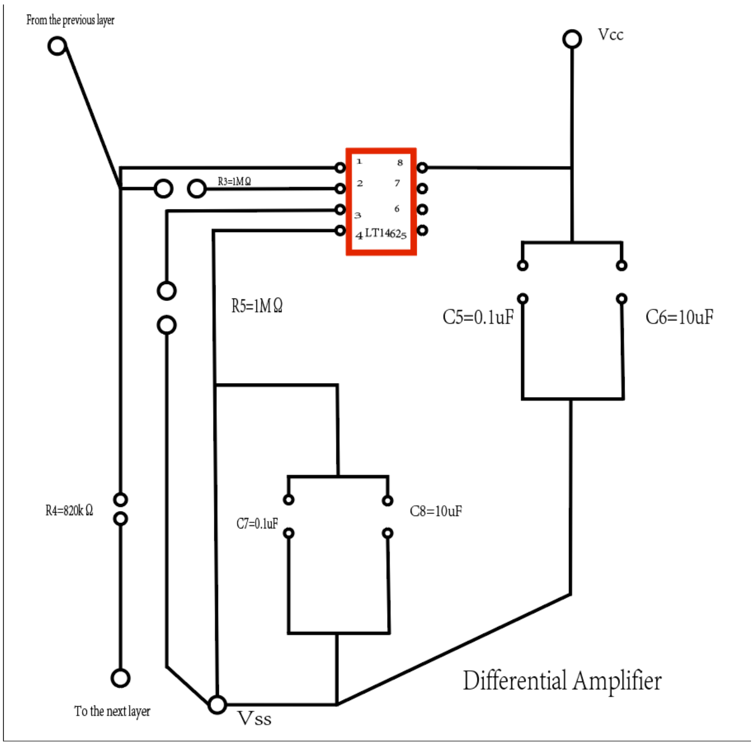

Figure 63 Differential Amplifier in AI

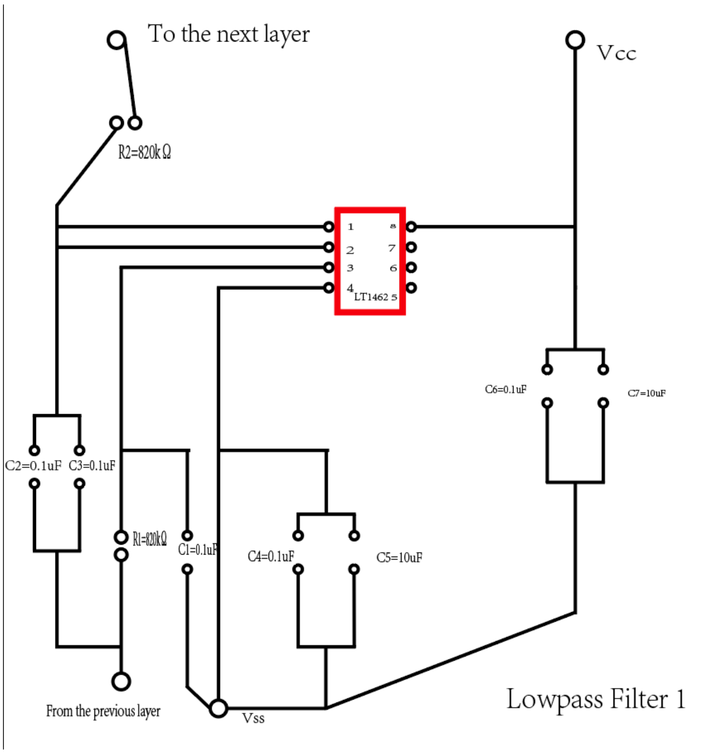

Figure 64 Low-pass filter first stage in AI

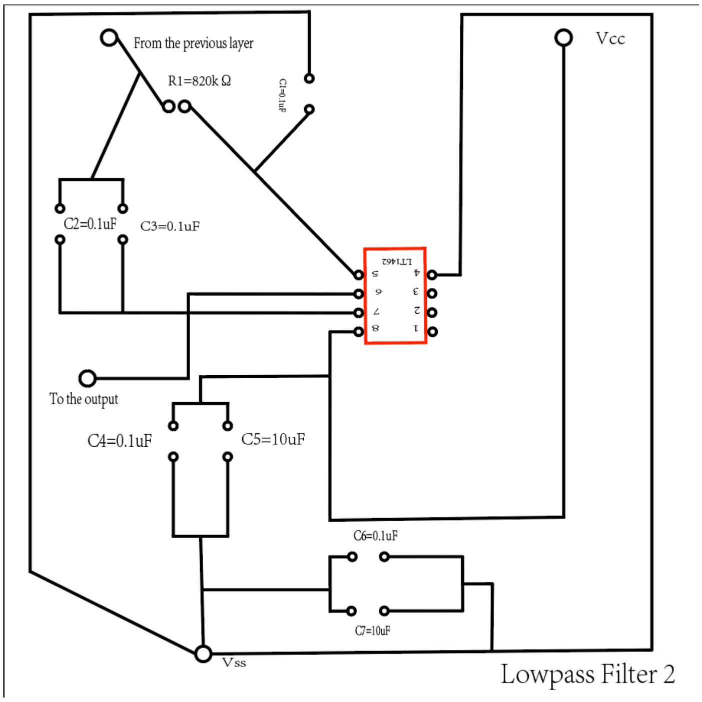

Figure 65 Lowpass Filter Second Stage in AI

The four pictures above are the circuit board diagrams that I draw with Adobe Illustrator. Because Dimatix material printer can recognize the image drawn by this software. The lines in the figure are the arrangement of wires, and each layer is a functional circuit. This work is also expected to be completed in future work. Of course, the circuits printed by this method will definitely have various problems after being connected together, such as interference between different layers. Eliminating interference between circuits is also the focus of future work.

Furthermore, the accuracy of LED display modules driven by Arduino also needs to be improved. The current accuracy is five thousandths, and the level of the last output voltage of the device is in the millivolt level, so higher accuracy is required. However, the Arduino Uno microcomputer may not be enough to support such high accuracy. In the future work, the Arduino Mega, an MCU with higher performance, will be used to complete the demonstration.

In addition, 3D printing technology can also be used to make a suitable case for all hardware devices completed by my research project. The requirements for this case include:

1. All modules must be able to be placed, including electrodes, circuits, charging and display modules.

2. Need to reserve a port to replace the power supply battery.

3. The electrode is located below the case in contact with the skin, and the display module is located above for easy observation.

10.2 Prospect of Project

The prospect of this research project is very broad, not just as a wearable device. The detection object of the wearable device proposed by this feasibility study is not just sweat, it can be all body fluids, such as urine, tears, saliva and blood, etc. The body fluid contains a lot of substances, which are closely related to the health of the human body. For example, glucose in body fluids is associated with diabetes, and the content of lactate can be used to prevent asthma and muscle weakness.

With the equipment under this system, only one type of electrode can be changed to measure many different substances with one equipment. In other words, the device can be made into a modular equipment. When special measurement of a certain substance is needed, it only needs to be replaced with a special electrode of the substance, without changing other parts of the device. This can maximize the use value of a device and reduce the cost of people's home or portable, wearable detection.

Appendix

Code of Arduino IDE

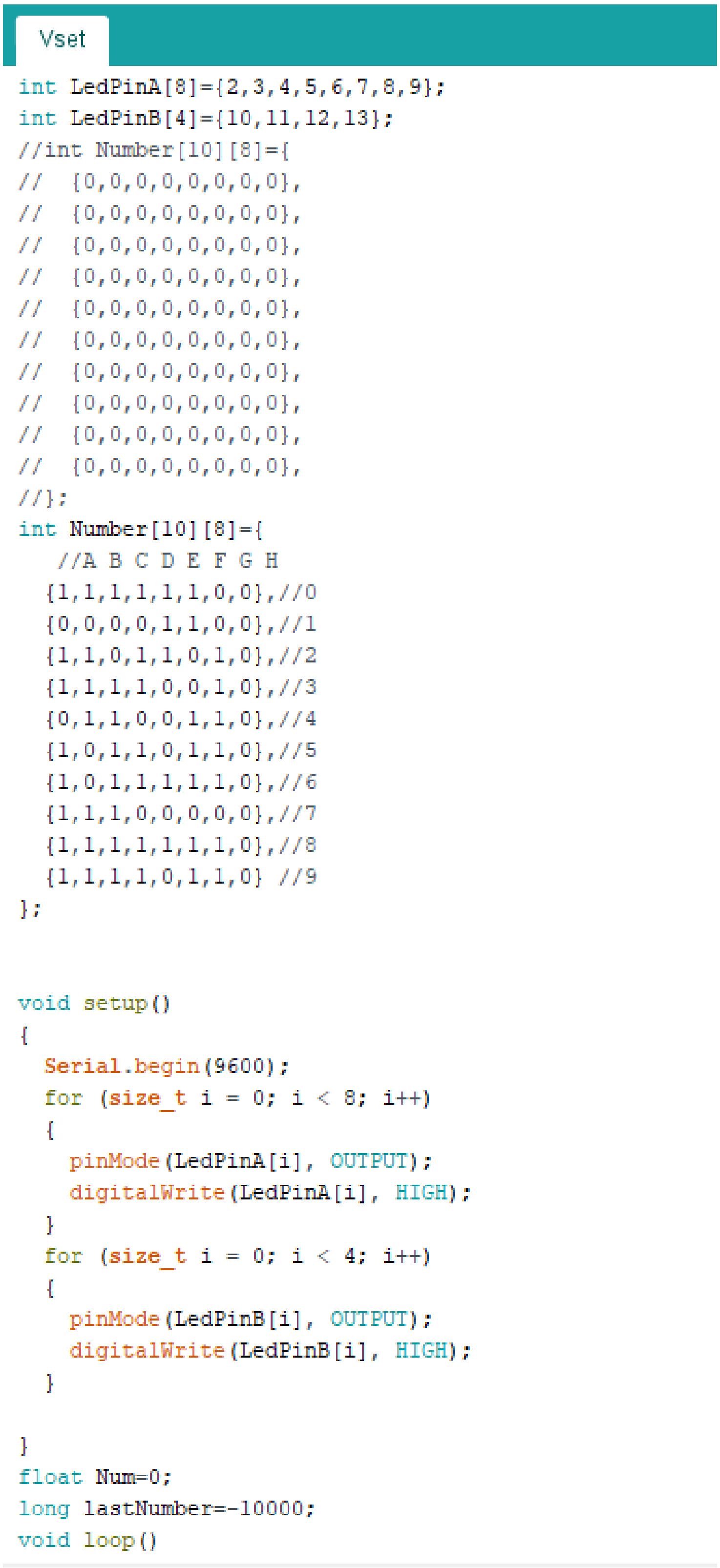

```
int LedPinA[8]={2,3,4,5,6,7,8,9};
int LedPinB[4]={10,11,12,13};
//int Number[10][8]={
//  {0,0,0,0,0,0,0,0},
//  {0,0,0,0,0,0,0,0},
//  {0,0,0,0,0,0,0,0},
//  {0,0,0,0,0,0,0,0},
//  {0,0,0,0,0,0,0,0},
//  {0,0,0,0,0,0,0,0},
//  {0,0,0,0,0,0,0,0},
//  {0,0,0,0,0,0,0,0},
//  {0,0,0,0,0,0,0,0},
//  {0,0,0,0,0,0,0,0},
//};
int Number[10][8]={
   //A B C D E F G H
  {1,1,1,1,1,1,0,0},//0
  {0,0,0,0,1,1,0,0},//1
  {1,1,0,1,1,0,1,0},//2
  {1,1,1,1,0,0,1,0},//3
  {0,1,1,0,0,1,1,0},//4
  {1,0,1,1,0,1,1,0},//5
  {1,0,1,1,1,1,1,0},//6
  {1,1,1,0,0,0,0,0},//7
  {1,1,1,1,1,1,1,0},//8
  {1,1,1,1,0,1,1,0} //9
};


void setup()
{
  Serial.begin(9600);
  for (size_t i = 0; i < 8; i++)
  {
    pinMode(LedPinA[i], OUTPUT);
    digitalWrite(LedPinA[i], HIGH);
  }
  for (size_t i = 0; i < 4; i++)
  {
    pinMode(LedPinB[i], OUTPUT);
    digitalWrite(LedPinB[i], HIGH);
  }

}
float Num=0;
long lastNumber=-10000;
void loop()
```

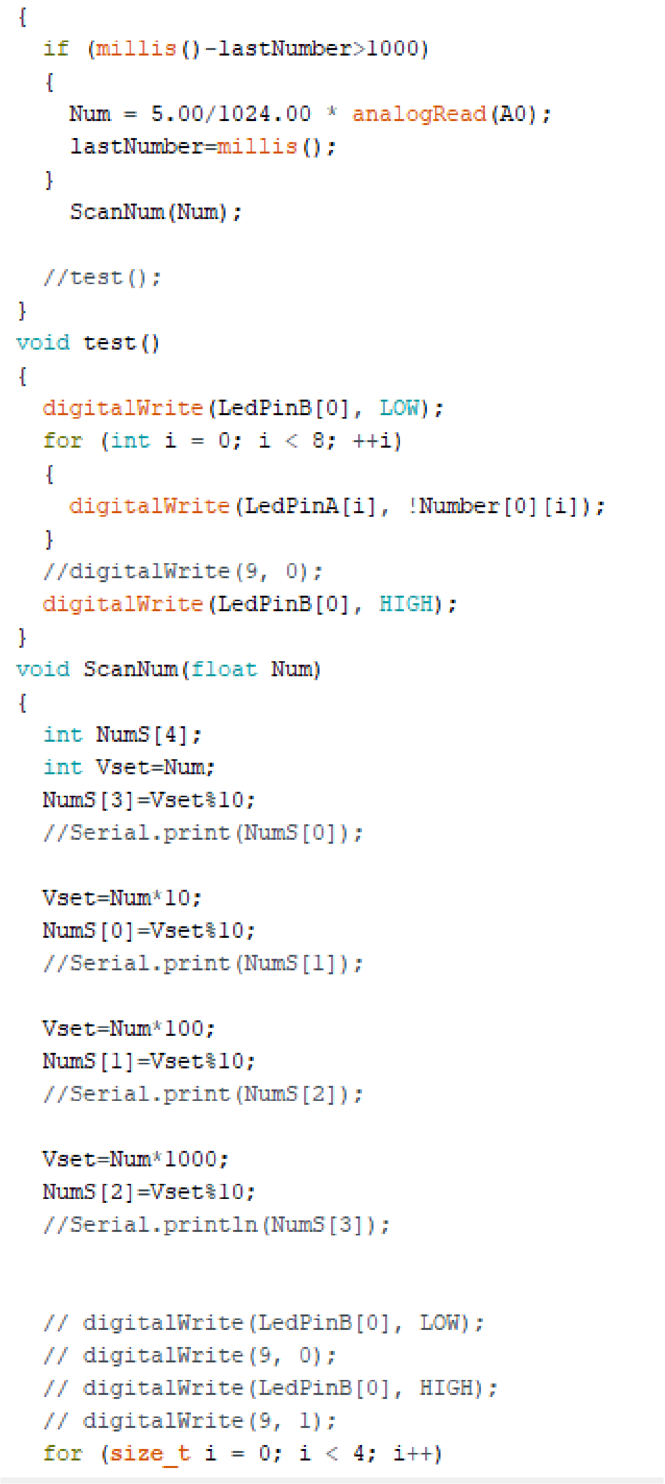

```
{
  if (millis()-lastNumber>1000)
  {
    Num = 5.00/1024.00 * analogRead(A0);
    lastNumber=millis();
  }
    ScanNum(Num);

  //test();
}
void test()
{
  digitalWrite(LedPinB[0], LOW);
  for (int i = 0; i < 8; ++i)
  {
    digitalWrite(LedPinA[i], !Number[0][i]);
  }
  //digitalWrite(9, 0);
  digitalWrite(LedPinB[0], HIGH);
}
void ScanNum(float Num)
{
  int NumS[4];
  int Vset=Num;
  NumS[3]=Vset%10;
  //Serial.print(NumS[0]);

  Vset=Num*10;
  NumS[0]=Vset%10;
  //Serial.print(NumS[1]);

  Vset=Num*100;
  NumS[1]=Vset%10;
  //Serial.print(NumS[2]);

  Vset=Num*1000;
  NumS[2]=Vset%10;
  //Serial.println(NumS[3]);


  // digitalWrite(LedPinB[0], LOW);
  // digitalWrite(9, 0);
  // digitalWrite(LedPinB[0], HIGH);
  // digitalWrite(9, 1);
  for (size_t i = 0; i < 4; i++)
```

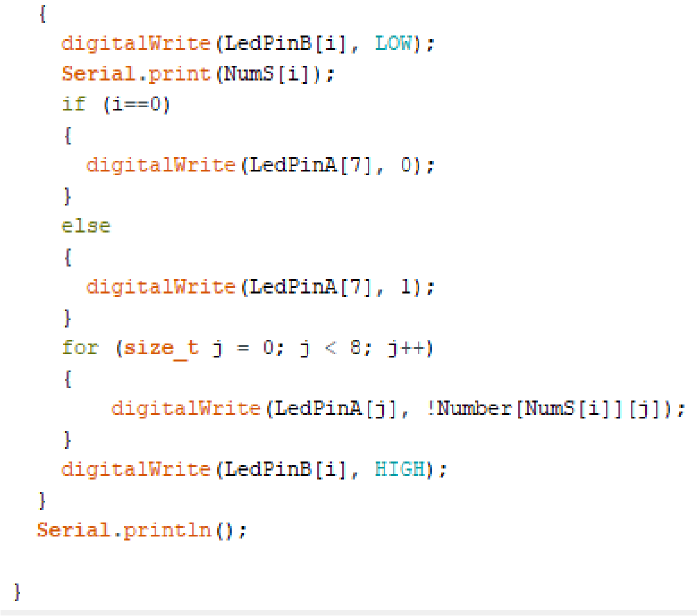

```
  {
    digitalWrite(LedPinB[i], LOW);
    Serial.print(NumS[i]);
    if (i==0)
    {
      digitalWrite(LedPinA[7], 0);
    }
    else
    {
      digitalWrite(LedPinA[7], 1);
    }
    for (size_t j = 0; j < 8; j++)
    {
        digitalWrite(LedPinA[j], !Number[NumS[i]][j]);
    }
    digitalWrite(LedPinB[i], HIGH);
  }
  Serial.println();

}
```

Reference List

---

[1] Jadoon S, Karim S, Akram M R, et al. Recent developments in sweat analysis and its applications [J]. International Journal of Analytical Chemistry, 2015, 2015.

[2] Barron E S G, Harrop G A. Studies on blood cell metabolism II. The effect of methylene blue and other dyes upon the glycolysis and lactic acid formation of mammalian and avian erythrocytes [J]. Journal of Biological Chemistry, 1928, 79(1): 65-87.

[3] Mena-Bravo A, De Castro M D L. Sweat: A sample with limited present applications and promising future in metabolomics [J]. Journal of Pharmaceutical and Biomedical Analysis, 2014, 90: 139-147.

[4] Sato K. Reviews of Physiology, Biochemistry and Pharmacology (Springer, 1977), Vol. 79, pp. 51–131.

[5] Wilke K, Martin A, Terstegen L, and Biel S S. A short history of sweat gland biology, International Journal of Cosmetic Science, 2007, 29, 169–179.

[6] Hung K, Zhang Y T, Tai B. Wearable medical devices for tele-home healthcare[C]//The 26th Annual International Conference of the IEEE Engineering in Medicine and Biology Society. IEEE, 2004, 2: 5384-5387.

[7] Hassanalieragh M, Page A, Soyata T, et al. Health monitoring and management using Internet-of-Things (IoT) sensing with cloud-based processing: Opportunities and challenges[C]//2015 IEEE International Conference on Services Computing. IEEE, 2015: 285-292.

[8] Denisevich P, Willman K W, Murray R W. Unidirectional current flow and charge state trapping at redox polymer interfaces on bilayer electrodes: principles, experimental demonstration, and theory[J]. Journal of the American Chemical Society, 1981, 103(16): 4727-4737.

[9] Carrish J J. Three electrode system in the generation of electrostatic images: U.S. Patent 4,160,257[P]. 1979-7-3.

[10] Gao W, Emaminejad S, Nyein H Y Y, et al. Fully integrated wearable sensor arrays for multiplexed in situ perspiration analysis[J]. Nature, 2016, 529(7587): 509-514.

[11] Schmuckler J S. Solubility product constant, Ksp[J]. Journal of Chemical Education, 1982, 59(3): 245.

[12] Pungor E, Tóth K. Ion-selective membrane electrodes. A review[J]. Analyst, 1970, 95(1132): 625-648.

[13] Cadogan A M, Diamond D, Smyth M R, et al. Sodium-selective polymeric membrane electrodes based on calix [4] arene ionophores[J]. Analyst, 1989, 114(12): 1551-1554.

[14] Rastogi N, Mehra R. Analysis of butterworth and chebyshev filters for ecg denoising using wavelets[J]. IOSR Journal of Electronics and Communication Engineering (IOSR-JECE), 2013, 6(6): 37-44.

[15] Strong, A., & Hoskins, K. R. (1996). LT1462/LT1463/LT1464/LT1465: Micropower dual and quad JFET op amps feature pA input bias currents and C-load (TM) drive capability. EDN, 41(18), 105-106.

[16] Graf, R. F. (1996). Converter and filter circuits. Elsevier.

[17] Teikari, P., Najjar, R. P., Malkki, H., Knoblauch, K., Dumortier, D., Gronfier, C., & Cooper, H. M. (2012). An inexpensive Arduino-based LED stimulator system for vision

research. Journal of Neuroscience Methods, 211(2), 227-236.